UNIVERSITY OF MINNESOTA
ST. ANTHONY FALLS HYDRAULIC LABORATORY

Technical Paper No. 50, Series B

Tandem Interference Effects for Noncavitating and Supercavitating Hydrofoils

by

J. M. WETZEL

Prepared for
OFFICE OF NAVAL RESEARCH
Department of the Navy
Washington, D.C.
under
Contract Nonr 710(24), Task NR 062-052

January 1965
Minneapolis, Minnesota

UNIVERSITY OF MINNESOTA
ST. ANTHONY FALLS HYDRAULIC LABORATORY

Technical Paper No. 50, Series B

Tandem Interference Effects for Noncavitating and Supercavitating Hydrofoils

by

J. M. WETZEL

Prepared for
OFFICE OF NAVAL RESEARCH
Department of the Navy
Washington, D.C.
under
Contract Nonr 710(24), Task NR 062-052

January 1965
Minneapolis, Minnesota

ABSTRACT

Experimental studies had previously been made at this Laboratory to determine the tandem interference effects for noncavitating hydrofoils. The results are compared with theory in this report, and good agreement is shown to exist. The experimental studies have now been extended to include fully submerged, ventilated foils of finite span. Both forced and naturally ventilated foils were employed in various configurations. The surface wave generated by the ventilated foil and the total interference effect of the forward foil on the force and cavity characteristics of the aft foil were of particular interest. The surface wave generated by the forward foil had relatively little influence on the force and cavity characteristics of the aft foil. For forced-ventilated foils, considerable change due to interference effects was observed in the cavity pressure of the aft foil. For long initial cavities on the forward and aft foil, the interference effect on the forces was relatively small, whereas for small initial cavities, the interference effect was much larger. Similar trends were observed for the naturally ventilated foils. Lateral separation of the forward foils reduced the interference effects to essentially negligible values.

CONTENTS

LIST OF ILLUSTRATIONS

LIST OF SYMBOLS

AR - aspect ratio

b - semi-span of rear foil

c - foil chord

C_D - drag coefficient

C_L - lift coefficient

f - submergence of foil leading edge below the undisturbed water surface

g - acceleration of gravity

J_1 - Bessel function of the first kind of order one

K_o - g/V^2

M_1 - non-dimensional strength of source

P_c - cavity pressure

P_o - free stream pressure

S - planform area

s - semi-span of forward foil

V - velocity

x - longitudinal distance from leading edge of forward foil

y - lateral distance from longitudinal centerline of foil system

z - vertical distance from undisturbed free surface to point in fluid. Positive z is directed upward.

α - geometric angle of attack

α_e - effective angle of attack

ϵ - downwash angle

θ - wave direction angle measured from fore and aft direction to the normal to a wave element

ρ - fluid density

σ - cavitation number, $\dfrac{P_o - P_c}{\frac{1}{2}\rho V^2}$

Subscripts

f - refers to forward foil

a - refers to aft foil

o - refers to single foil with no interference effects

x - indicates variation of parameter with longitudinal foil spacing

TANDEM INTERFERENCE EFFECTS FOR NONCAVITATING AND SUPERCAVITATING HYDROFOILS

I. INTRODUCTION

In the design of hydrofoil craft, problems arise concerning the spacing of the foils in the longitudinal and lateral directions. The desired inherent stability of the craft will dictate certain basic requirements to be satisfied. For a comprehensive design, some knowledge of the interference effects between two or more foils should be available. The interference problem associated with the use of hydrofoils in a tandem configuration is similar to the wing-tail interference problem in aerodynamics but is further complicated by the existence of a free surface and the generation by the foils of waves on the free surface. In the case of supercavitating foils, interference effects may also be experienced from the rather large trailing cavity and the associated wake.

Some theoretical work has been done to predict the downwash effects created by both noncavitating and supercavitating foils [1, 2].* In an earlier report from this Laboratory [3], experimental studies were described relative to the interference effect for two identical, fully submerged, flat, noncavitating hydrofoils in tandem moving through smooth water. A limited number of the experimental results were compared in Ref. [3] with a theory for three-dimensional foils at a finite submergence in a fluid of infinite depth [1]. The theory indicated values of downwash angle which appeared to be somewhat higher than those determined from the experimental data. There was excellent agreement as to the location of points of maximum and minimum downwash, indicating the value of the theory in the determination of the optimum location of the rear foil of a tandem system.

Following the publication of Ref. [3], more extensive computations of downwash angle were made using a digital computer. The results of these computations were compared with the data and were presented in an earlier memorandum [4] which received only limited distribution. In order to make this information more generally available, it is included in the present report.

Experimental studies have also been undertaken for ventilated, fully submerged, flat plate hydrofoils of finite span. Most of the data for these

*Numbers in brackets refer to the List of References on page 23.

foils was taken utilizing forced-ventilated conditions. Some measurements were made of the surface wave generated by a single, ventilated foil for various flow conditions. Experiments were also conducted to determine the interference effects for two split forward foils and a single foil aft as well as for single foils forward and aft. A limited amount of data was taken with foils ventilated to the atmosphere by means of a base vented strut piercing the free surface.

The investigation was carried out under the sponsorship of the Office of Naval Research, under terms of Contract Nonr 710(24), Task NR 062-052.

II. GENERAL CONSIDERATIONS

For reference purposes, the theoretical equations are presented for the mean downwash velocity behind a flat, noncavitating hydrofoil of finite span. The theory for three-dimensional foils in a fluid of infinite depth with a free surface is based on a velocity potential which is the sum of four potentials. The first is the potential for a finite span foil in an infinite fluid (no free surface), the second is the potential for the biplane image reflection in the free surface of the original foil, the third is a potential that arises because of wave formation at the free surface, and the fourth is a correction potential introduced to insure that all boundary conditions are satisfied. In the evaluation of the mean downwash velocity an elliptical distribution of circulation was assumed for the foil. Due to the neglect of certain terms in the derivation, the theory is invalid in the immediate vicinity of the foil, and it is expected that it will give poorest agreement with experimental data taken at low speeds.

To allow some correction for the rollup of the tip vortices, it was assumed that if the aft foil of a tandem system had the same span as the forward foil, the average value of the downwash was essentially the same as the value at midspan. It was further assumed that the correction commonly applied in classical airfoil theory for the variation of downwash along the longitudinal x-axis in the plane of the foil may also be applied at any point in the same horizontal plane as the foil. The theory would thus be most accurate when the submergences of the fore and aft foils of the tandem system are equal.

The equation obtained for the downwash angle parameter (ϵ / C_L), expressed in radians, is

$$\frac{\epsilon}{C_L} = \frac{c}{\pi b s}\left\{ b - \left\{ [(f+z)^2 + s^2 - b^2]^2 + 4(f+z)^2 b^2 \right\}^{1/4} \sin\beta' \right\}$$

$$- \frac{2c}{\pi b}\int_0^{\pi/2} \mathrm{Exp}[K_o(z-f)\sec^2\theta]\frac{\sec\theta\, J_1(K_o s\sec^2\theta\sin\theta)\,\sin(K_o b\sec^2\theta\sin\theta)}{\sin^2\theta}d\theta$$

$$+ \frac{4c}{\pi b}\int_0^{\pi/2} \mathrm{Exp}[K_o(z-f)\sec^2\theta]\frac{\sec\theta\, J_1(K_o s\sec^2\theta\sin\theta)\,\sin(K_o b\sec^2\theta\sin\theta)\cos(K_o x\sec\theta)}{\sin^2\theta}d\theta$$

(1)

where

$$\sin\beta' = \left\{\frac{1}{2}\left\{1 - \frac{(f+z)^2 + s^2 - b^2}{\sqrt{[(f+z)^2 + s^2 - b^2]^2 + 4(f+z)^2 b^2}}\right\}\right\}^{1/2}$$

It was shown that for high speeds the second term in the expression for ϵ/C_L [Eq. (1)] may be approximated by

$$-\frac{c}{\pi s}\left\{1 - \frac{(f-z)/s}{\sqrt{1 + (\frac{f-z}{s})^2}}\right\} \qquad (2)$$

where ϵ = downwash angle, taken as positive when it results in a reduction of the angle of attack,

C_L = $2L/\rho SV^2$, the lift coefficient for the forward foil corresponding to its geometric angle of attack,

c = chord of forward foil,

ρ = fluid density,

S = hydrofoil planform area,

V = forward speed of hydrofoil system,

b = semi-span of rear foil,

s = semi-span of forward foil,

f = submergence of forward foil below the undisturbed surface,

x, y, z = coordinates of any point in the fluid measured from a right-handed set of axes whose origin is in the plane of the undisturbed free surface and directly above the forward foil lifting line. Positive z is directed upward. Hence, for the submergence of the rear foil substitute a negative value for z,

$K_o = g/V^2$, a wave number,

g = acceleration of gravity,

θ = wave direction angle measured from the fore-and-aft direction to the normal to a wave element, and

$J_1(K_o s \sec^2\theta \sin\theta)$ = Bessel function of the first kind of order one and argument $K_o s \sec^2\theta \sin\theta$.

The high speed approximation [using Eq. (2) for the second term of Eq. (1)] was found to differ very little from the evaluation of Eq. (1) even at a velocity of 5 fps. The downwash angle parameter was therefore computed using the high speed approximation in all other cases.

The first two terms of Eq. (1) are readily computed with a desk calculator and the integrand in the third term was evaluated using an IBM digital computer. The program was written in Fortran language. The expression was evaluated for various velocities (5, 10, and 15 fps), submergences of the forward foil (f = 1 chord, f = 2 chords), submergences of the rear foil (z = -1 chord, -2 chords, and -3 chords), and longitudinal spacings of the foils (4, 8, 12, 16, 20, 24, 28, 32, 36, and 40 chords). The expression was evaluated every 0.25 degree from $\theta = 0$ degrees to $\theta = 90$ degrees and integrated between these limits. Combining the value of this integral with the first two terms of the high speed approximation then gave the theoretical value of the downwash angle parameter in radians. The theoretical curves obtained in this manner are compared with the experimental data in Section IV.

Theoretical work has also been carried out by Yim [2] for supercavitating foils submerged beneath a free surface. Both two- and three-dimensional cavities were considered. In this linearized theory, it was assumed that the downwash at a considerable distance downstream of the cavity was essentially independent of the shape of the foil. This permitted the separation of the downwash distribution into two parts: the downwash from the vortex distribution, and the downwash due to the cavity itself in the presence of the free surface. The lifting line theory by Kaplan, Breslin, and Jacobs [1] was used for the first part of the problem, and this theory has been reasonably verified by experimental data as shown in Section IV-A of this paper. Yim was thus primarily concerned with a determination of the downwash angle associated with the cavity alone. The mathematical model of the cavity consisted of a uniform source plus a line sink to satisfy the closure requirement for the cavity. A number of numerical calculations were presented to relate a non-dimensional downwash parameter, ϵ/M_1, and the Froude number based on foil submergence. The parameter, M_1, is a non-dimensional expression for the strength of the source, and ϵ is the downwash angle expressed in radians. These calculations were made for a number of distances aft of the foil as well as for different cavity lengths. Numerical computations were also made for foils of different aspect ratios. A considerable difference in the flow field downstream of the cavity was found to exist for various aspect ratio foils. Cavity length also appeared to create a significant variance in the downwash pattern.

The downwash due to the cavity was thus determined to be a function of Froude number, foil submergence, distance aft of the foil, size of the cavity, and aspect ratio. The size of the cavity is related to the parameter M_1. It was suggested that some indication of the order of magnitude of M_1 could be determined by means of the point drag cavity model, although difficulties have been experienced in the application of this method to the experimental data presented in this report.

III. EXPERIMENTAL APPARATUS AND PROCEDURE

A. Towing Facility

The experimental tests were conducted in the St. Anthony Falls Hydraulic Laboratory towing tank, which is 9 ft wide and 220 ft long. The tank was filled with water to a depth of 4.5 ft. The self-propelled towing carriage is capable of attaining a maximum speed of 25 fps, although lower speeds were used during the tests to permit a sufficient length of test run.

B. Foils and Instrumentation

(1) Noncavitating Foils

Two identical foils of zero dihedral angle and rectangular planform were used. The foils were machined from aluminum to a NACA 16-509 section. The pressure distribution for this section is rather uniform across the chord and thus the section is well suited for practical applications. Each foil had a chord of 3 in. and a span of 18 in. (Æ = 6) and was attached at midspan to a strut of 3-in. chord machined to a NACA 16-012 section.

(2) Ventilated Foils

The foils were machined from aluminum to a wedge section with an angle of 6 degrees. Both upper and lower surfaces were flat, terminating in a sharp leading edge. The foils had a 3-in. chord, 6-in. span, zero dihedral angle, and rectangular planform. A similar foil with a 3-in. chord and 18-in. span was also used for a special group of tests.

Attachment was made at midspan to a streamlined supporting strut of 2-in. chord with the leading edge of the strut 1 in. behind the leading edge of the foil. Ventilating air was introduced to the upper surface of the foil by means of a supply tube through the strut near the mid-chord position of the foil. This tube terminated in ports at the base of the strut so that the air moved spanwise across the upper surface of the foil. The air flow rate to the foil was determined by a calibrated orifice meter placed in the supply line. The cavity pressure was measured with a Statham pressure transducer connected by a liquid-filled tube passing through the strut to a diaphragm on the upper surface of the foil near the trailing edge. The pressure transducer was mounted above the water surface.

A brief series of tests was also conducted with the same foils ventilated to the atmosphere. In this case the streamlined strut used previously was replaced with a parabolic, base vented strut to provide an external air path to the foil. As the cavity on the foil was thus opened to the atmosphere, it was assumed that the cavity pressure was atmospheric.

(3) Instrumentation

Lift and drag forces were measured with a two-component strain gage dynamometer. The lift and drag were measured perpendicular and parallel to the direction of motion of the tandem assembly, respectively, rather than perpendicular and parallel to the instantaneous velocity vector. Forces were continuously recorded during the test run on a Sanborn 4-channel recorder.

The profile of the surface wave generated by the ventilated foil was measured using the Laboratory sonic wave transducer [5]. The sonic head was attached to a subcarriage that permitted movement with respect to the main carriage in both the lateral and the longitudinal directions. The rails of the subcarriage were fixed to the underside of the main towing carriage. The movement of the subcarriage in the longitudinal direction was detected by a potentiometer attached to a wheel of the subcarriage. The signal from the potentiometer was fed to one input of a Mosely XY recorder, and the output from the sonic transducer was fed to the other input of the recorder. It was thus possible to obtain a trace of the wave profile in the longitudinal direction, independent of the speed at which the subcarriage was moved during the run. By locating the sonic head at various lateral positions from the centerspan of the foil, a mapping of the water surface was readily obtained. A photograph of the towing carriage and the subcarriage is shown in Fig. 1.

C. Experimental Procedure

Force measurements were first made for a single foil for various velocities, angles of attack, submergences, and in the case of the ventilated foils, cavitation numbers. To determine the total interference effect on the force characteristics, the aft foil of the tandem configuration was attached to the dynamometer which could be moved in the longitudinal direction. A definition sketch is shown in Fig. 2. This sketch shows force ventilated foils. For the noncavitating foils, σ does not apply, and as only a single forward foil was used, $y = 0$. The foils were set at particular angles of attack and submergences, and the lift and drag forces were measured for given velocities and separations of the foils. For tests with noncavitating foils, the rear foil was essentially used as a downwash meter. Using the previously obtained lift curve for the single foil and the measured lift coefficient for the aft foil in the tandem configuration, the effective angle of attack for the aft foil was obtained. The difference between the effective angle of attack thus determined, α_e, and the geometric angle of attack, α, gave the downwash angle, ϵ, defined as positive when it resulted in a reduction in the angle of attack, i. e.,

$$\epsilon = \alpha - \alpha_e$$

For the force ventilated foils, the air flow rate to each of the foils was held constant to predetermined values during the test run. The interference effect also apparently caused a change in the air entrainment characteristics which created additional complications, as will be discussed in a later section.

IV. DISCUSSION OF RESULTS

A. Downwash Angle for Noncavitating Foils

The experimental data for the downwash angle, ϵ, are presented in Figs. 3 to 8. Each of these figures shows data for a fixed submergence of the forward foil and a given towing velocity, the submergence of the aft foil varying from one to three chords. The geometric angles of attack for both the forward and aft foil were 4 degrees. The downwash angle in degrees has been divided by the lift coefficient and plotted as a function of the foil separation in the longitudinal direction. The method used in measuring the downwash angle resulted in an average value across the span of the aft foil. The solid line in each of the figures is the theoretical value calculated from Eq. (1) using the approximation for high speeds as given in Eq. (2).

From Figs. 3, 4, and 5 it is apparent that the downwash angle varies with foil separation in an oscillating manner. The greatest variation is indicated at the lower velocities. It has been shown previously [3] that this variation is associated with the surface wave generated by the foil. In general, the points of maximum and minimum downwash are predicted quite well by the theory. It may be noted, however, that in some instances the experimental data deviated somewhat from the theoretical curves. This deviation can be seen in Figs. 3b, 3c, 4b, 5b, and 5c. The experimental data have been checked and the reason for the discrepancy is not known. The greatest variation of downwash angle with foil separation was found for the condition where both the forward and aft foil were at the same submergence. In Figs. 6, 7, and 8 data are shown for the forward foil at a two chord submergence with the submergence of the aft foil varying from one to three chords. The same general trends are observed, in that good agreement is obtained with regard to location of the maximum and minimum downwash angles. The greatest deviation of the data from the theoretical curve is found at a velocity of 5 fps (Fig. 6) and two and three chord submergence of the aft foil. At the higher velocities (Figs. 7 and 8), excellent agreement is obtained.

B. Surface Waves Generated by a Single, Ventilated Foil

(1) Force and Cavity Characteristics for a Single Foil

It was first of interest to determine the force and cavity characteristics of a single forced-ventilated foil for various angles of attack and cavitation numbers. Plots of the lift and drag coefficients, based on the planform area, as a function of cavitation number are shown in Figs. 9a and b. The solid lines shown are drawn as visual averages through the experimental data. These results were obtained with the foil at a one chord submergence. Photographs of the cavity were taken for angles of attack of 14 and 18 degrees. These photos were used to obtain the planform shape and length of the cavity. Cavity lengths scaled from the negatives are plotted in Fig. 9c as a function of σ. The cavity length was taken as the distance from the leading edge of the foil to the tail of the cavity. The cavitation number was based on the measured cavity pressure and the cavity length has been made non-dimensional with respect to the foil chord.

(2) Surface Wave Measurements

The generation of a surface wave by a submerged, ventilated foil is considerably more complex than that for a fully wetted foil. The characteristics of the cavity attached to the foil contribute to the deformation of the free-surface; thus the cavitation number is also of importance. Experimental measurements were made for the conditions listed in Table I.

TABLE I

$\alpha = 14^{\circ}$ f = 1 chord		$\alpha = 18^{\circ}$ f = 1 chord		$\alpha = 18^{\circ}$ f = 2 chords	
V (fps)	σ	V (fps)	σ	V (fps)	σ
10	0.102	10	0.114	10	0.147
10	0.203	10	0.173	10	0.180
14	0.072	10	0.264	10	0.303
14	0.209	14	0.080	14	0.103
14	0.292	14	0.198	14	0.205
18	0.049	14	0.333	14	0.352
		18	0.059	18	0.072

The angle of attack was measured with respect to the underside of the foil. Submergence was taken as the vertical distance from the smooth water surface to the leading edge of the foil. Original intentions were to obtain data for three cavitation numbers at each velocity, but in most instances this was difficult to accomplish. Data for short cavities were particularly limited as a transient behavior was found that did not decay rapidly enough to permit obtaining a profile of the surface wave under the desired steady conditions. Also, it was not possible to obtain precisely the same value of the cavitation number for the various foil geometries. However, values were used that resulted in relatively long, intermediate, and short cavities.

Longitudinal profiles of the water surface were taken at transverse distances of 0 to 28 in. from the centerline of the foil at 4-in. intervals. For some tests, profiles were also taken at 2 and 6 in. from the centerline. The wave pattern was assumed to be symmetrical about the span centerline; therefore, measurements were made only to one side of the foil strut. A record was first obtained of the smooth water surface to establish a reference line for all other elevations. After a series of profiles were taken for a given set of conditions, contour maps were drawn based on these longitudinal profiles. The contour method of representing the wave pattern was selected to give an overall impression as to the severity and extent of the disturbance for various conditions. Data reduced in this manner are shown in Fig. 10 for the variables listed in Table I. The contour interval for these plots is 0.1 inch. Contours representing elevations below the mean water surface are shown with dashed lines, and those representing elevations above the mean water surface are shown with solid lines. The reference or zero contour corresponds to the elevation of the mean water surface. Photographs of the cavity have also been obtained for some of the test conditions. The planform shape of the cavity scaled from the available photographs has been sketched on the appropriate figures and has been shaded with dots for emphasis. The semi-span of the foil is indicated by hatching. It should also be noted that the ordinate of these figures has been drawn to a different scale than the abscissa to avoid excessive crowding of the contour lines. The leading edge of the foil is shown 3.33 chords from the reference line. In some cases the contour lines have been terminated on the map. This corresponds to the limit of the region at which reliable measurements were obtained. Thus, extrapolations were not made into areas for which data were not available.

A comparison of the contours in Figs. 10a and 10b shows the effect on the wave pattern of doubling σ at a velocity of 10 fps, and a comparison of Figs. 10c and 10d shows the effect of nearly tripling σ at a velocity of 14 fps. It will be noted in Figs. 10a and 10b that the wave length is essentially the same, and the decrease in cavity size results in a decrease in the local disturbance in the region of the foil and cavity. The wave amplitude aft of the foil apparently increases with the cavitation number, primarily through an increase in the lift coefficient.

The surface wave pattern changes somewhat at the higher velocity, as shown in Figs. 10c and 10d. The wave amplitude also is greater than at a velocity of 10 fps. A direct comparison of Figs. 10b and 10d will serve as an example. The cavitation numbers and lift coefficients are essentially the same for both plots. Only the velocity has varied appreciably. The change in the amplitude is apparent. A further increase in σ and C_L for the same velocity results in an additional increase in the wave amplitude as shown in Fig. 10e. A large cavity at a high velocity creates a comparatively large local disturbance (Fig. 10f).

The remainder of the wave profiles were taken with the foil at an angle of attack of 18 degrees. The effect of increasing σ on the elevation of the water surface is shown in Figs. 10g, h, i, and 10j, k, and ℓ for velocities of 10 and 14 fps respectively. The same general trends are noted, and the large wave created by a foil operating at a large lift coefficient is apparent in Fig. 10ℓ. Figure 10m again shows the influence of a large cavity on the wave pattern.

All the previous wave patterns were a result of the foil at a one chord submergence. Figures 10n through 10t indicate the effect of increasing the foil submergence. The wave amplitudes have been considerably reduced in all cases, as the contributions of both the foil lift and the cavity size are diminished.

C. Tandem Interference Effects for Ventilated Foils

(1) <u>Single Foil Forward and Aft</u>

The first series of tests to determine the total interference effect for ventilated foils was conducted with two identical foils directly in line with each other in the longitudinal direction. This configuration corresponds to $y = 0$ in the definition sketch in Fig. 2 and it was chosen to represent maximum interference conditions. The particular procedure followed for these measurements is given below:

1. The force characteristics were determined for the aft foil at a σ established by a specified air supply rate to the cavity. The forward foil was removed from the water for these measurements.

2. With the aft foil removed, the forward foil was placed into the water at the specified submergence and angle of attack. The air supply rate was adjusted to provide essentially the same cavitation number as that previously measured for the aft foil.

3. The aft foil was placed in the water, and tests were made for various longitudinal separations of the foils. If no interference effect existed, the forces and the cavities should have been the same on both the forward and aft foils.

The procedures outlined above resulted in a measurement of the total interference effect. As previously mentioned, the interference may arise from several sources. A downwash velocity results from the lift generated by the forward foil and also from the size of the attached cavity in the presence of the free surface. Furthermore, it may be possible with small foil separations that the air entrainment characteristics are altered from those for the foil alone due to the increased turbulence of the flow.

The relationship between air supplied to the cavity and the cavitation number may be divided into two parts: where the air requirement is proportional to cavitation number (reentrant jet cavities), and where the air requirement is essentially independent of the cavitation number (non-reentrant jet cavities). In the former region, for a given cavitation number, the air requirements increase as the angle of attack is increased. In the latter region, the effect of angle of attack is relatively smaller. Thus, it is expected that the changes in cavitation number due to a given change in angle of attack (downwash angle) would be considerably larger at the larger cavitation numbers. This is based on the assumption that the air flow rate to the cavity is constant and that the air entrainment characteristics are not altered by interference effects. Alternatively, it may be considered that the downwash angle is zero and the air entrainment characteristics of the aft foil are different from those obtained for the foil alone. In that case, the change in cavitation number is also much greater at the higher cavitation number than at the lower values. Therefore, the use of forced ventilated foils increases the difficulty in actually assessing the magnitude of the downwash angle itself.

The conditions for which experimental measurements have been made with forced ventilated foils are listed in Table II. The subscripts, f and a, on the listed parameters refer to the forward and aft foil respectively.

TABLE II

α_f degrees	α_a degrees	σ_f	σ_a	f_f chords	f_a chords	V fps
14	14	0.05	0.05	1	1	18
14	14	0.053	0.063	1	2	18
14	14	0.06	0.06	1	1	14
14	14	0.072	0.073	1	1	14
14	14	0.06	0.165	1	1	14
14	14	0.068	0.210	1	1	14
14	14	0.207	0.208	1	1	14
18	18	0.337	0.354	1	1	14

The particular cavitation numbers selected for the tests were chosen to result in both non-reentrant jet and reentrant jet cavities, and the tabulated values are for each foil alone, i. e., without interference effects. Generally, for $\sigma > 0.1$, reentrant jet cavities were found to exist. Both cavity types were of interest, as the air entrainment characteristics are dependent on the type of cavity. It will be seen that the interference effects are also somewhat different.

The experimental data are plotted in Figs. 11a to 11h. In each of these figures, the lift coefficient, C_{L_x}, drag coefficient, C_{D_x}, and cavitation number, σ_x, of the aft foil have been divided by the corresponding value for the foil alone (denoted with the subscript zero). The parameters for the aft foil have been given a subscript x to indicate variation with foil separation. For the ordinate of the plots, the subscript a has been dropped to reduce complexity in notation. The cavitation numbers for the forward and aft foils alone are shown on the small sketch on each figure. The resulting ratios were plotted as a function of the longitudinal spacing of the foil expressed in chords, x/c.

On each plot for the lift coefficient in Fig. 11, two sets of symbols have been used. The open symbols represent the experimental data based on measurements of the total interference effect. The solid symbols represent the calculated lift coefficient for the aft foil, assuming that the entire interference effect is caused by a change in cavitation number, the effective angle of attack remaining the same as the geometric angle of attack in all cases. These points were added to provide an estimate of the interference effect resulting from a change in the air entrainment characteristics of the aft foil.

Figure 11a shows the experimental data for both forward and aft foils at the same submergence. The low cavitation numbers resulted in initially long cavities. The lift and drag coefficients for the aft foil changed very little with foil separation, whereas the cavitation number varied by a maximum of 50 per cent. As the initial σ for the aft foil was low, the 50 per cent increase in σ from 0.05 to 0.075 did not result in a large change in the forces. The interference effect essentially vanishes if the aft foil is submerged to two chords, as shown in Fig. 11b. Some variation of the drag coefficient persists with foil separation; this may be caused by changes in the strut drag.

At a velocity of 14 fps, similar results are obtained. However, as seen in Figs. 11c and 11d, the change in σ is somewhat greater, doubling at a foil separation of ten chords. This increase still does not affect the forces appreciably. In each of these figures, the measured lift coefficients are quite similar to those determined assuming the interference effect is dependent on the cavitation number, as indicated by the solid symbols.

A different trend is noted as the cavitation number of the aft foil is increased, maintaining the cavitation number of the forward foil essentially the same. Typical results are shown in Figs. 11e and 11f. In this case σ reaches a maximum at a twenty chord separation of the foils, rather than at the smallest separation as previously noted in Fig. 11d. The forces tend to follow this variation in cavitation number much closer than in the previous case, as the actual change in the cavitation number was greater. However, it can also be seen by a comparison of the open and solid symbols that apparently the effective angle of attack has been changed to some extent.

For air flow rates that resulted in shorter cavities on both the forward and aft foils, the interference effects are considerably different. Typical results are shown plotted in Figs. 11g and 11h for angles of attack of 14 and 18 degrees respectively. In both instances the cavitation number of the aft foil has been reduced rather than increased as noted in the previous figures. This reduction in cavitation number resulted in a lengthening of the cavity as observed during the tests. Again, a change in the angle of attack of the aft foil is evidently experienced, as the lift coefficients determined by the geometric angle of attack and cavitation number at each x/c are greater than those measured.

For a particular series of tests, several photographs were taken to obtain visual evidence of the tandem interference effect. Photographs were first taken of the forward and aft foils operating separately to provide a reference for the other conditions. Typical photographs are shown in Fig. 12 for the foils moving from right to left. As the camera was situated below and to one side of the cavity, the double image is created by a reflection in the water surface. Therefore, both the bottom surface (lower image) and the top surface (upper image) of the cavities can be seen. Note that the cavity lengths of both the forward (Fig. 12a) and aft foil (Fig. 12b) are essentially the same. Fig. 12c shows the foils in a tandem configuration at a longitudinal spacing of ten chords. The interference effect on the aft foil is quite extensive for this condition. The shortened cavity length on the aft foil indicates the change in the cavitation number, which has been increased from 0.08 to about 0.15. As the longitudinal foil spacing is increased to fifteen chords, less interference is noted as in Fig. 12d. In this photo, only the tail of the cavity from the forward foil is visible.

Closer inspection of Fig. 12c indicates that a very severe disturbance exists in the region of the aft foil for relatively small foil separations. The air entrained from the forward cavity flows over the aft foil, causing a disrupted flow pattern. In all the reported tests, the air flow to the aft foil was maintained the same as that previously established for the foil alone. That is, the air flow rate resulting in the cavity in Fig. 12b is the same as that in Fig. 12c. It is well known that for a single foil (no interference effects) a definite relationship exists between the air flow rate and the cavitation number, assuming other factors, such as the angle of attack and velocity, remain constant. If a foil is placed in a region where the turbulence is greatly increased, such as shown in Fig. 12c, it is possible that the relationship between air flow rate and cavitation number is no longer the same. It is expected that the increased turbulence may result in a larger air flow rate being required to maintain the same cavitation number. Conversely, if the air flow rate is not changed, then the cavitation number would be expected to increase.

It was also of interest to relate the tandem interference effect to the surface waves generated by the forward foil. This can be done directly with a comparison of Figs. 11a and 10f for essentially the same flow conditions. The origin of the abscissa of Fig. 10f must be shifted to the right about three chords to make the definitions of longitudinal separation the same. The cavity is approximately twelve chords long. The measurements of interference effects were started at a fifteen chord separation as shown in Fig. 11a. At this location, the aft foil is practically in the tail of the forward cavity itself; thus some influence of this disturbance on the aft cavity would certainly be expected. The cavitation number of the aft foil decreases with foil separation. At a longitudinal spacing of thirty chords the cavitation number is essentially the same as for an infinite separation. The wave pattern shown in Fig. 10f indicates that the aft foil has apparently been moved through a rather weak depression in the water surface over this range of separations. However, no definite oscillatory pattern corresponding to the wave profile can be detected as has been found previously for noncavitating foils.

A comparison can also be made between the wave pattern in Fig. 10c and the experimental data in Fig. 11c for a velocity of 14 fps. Again no oscillatory trend as evidenced in the wave profile along the centerline is observed in the variation of σ or the force coefficients.

In general, the variation of the force coefficients with both angle of attack and cavitation number, in addition to the inherent scatter in the experimental data, precluded any precise information relative to the actual downwash angle associated with a ventilated hydrofoil. In several attempts to reduce the data in this form, it was found that the comparatively small lift-curve slope for a ventilated foil was partially responsible for much of the scatter obtained when the downwash angle was determined by the method similar to that previously used for noncavitating foils [3]. It was thus decided to initiate a brief series of tests with a ventilated foil forward and a typical fully wetted section used for the aft foil. The aft foil was then used primarily as a downwash meter. The lift curve slope for the fully wetted aft foil was much greater than that for the ventilated foil previously used, and therefore the variation in lift for a given change in angle of attack was also greater. The cavitation number of the aft foil was also no longer a parameter. This resulted in more accurate measurements of the downwash angle than previously obtained. As the available theory [2] on the downwash angle for supercavitating foils was evaluated for foils of aspect ratio 6, a flat plate with a 3-in. chord and 18-in. span was employed as the ventilated forward foil in this series of tests. The noncavitating aft foil was of a NACA 16-509 section also with an aspect ratio of 6 (3-in. chord, 18-in. span) and was set at the same submergence as the forward foil (one chord). This foil was used in the earlier tests described in Ref. [3] and also for the experimental data presented in Figs. 3 through 8.

Experimental data taken for two velocities, two angles of attack, and various cavitation numbers are presented in Fig. 13. The downwash angle, ϵ, is expressed in radians. In Fig. 13a, three sets of data are shown. Two sets of data correspond to fully ventilated flow at the cavitation numbers as indicated, and the triangular symbols in Fig. 13a correspond to data taken with the forward foil in the fully wetted condition. The solid lines in Figs. 13a and 13b represent values calculated for fully wetted flow from Eq. (1), incorporating the high speed approximation. The experimental data for the sharp-edged foil in a fully wetted condition are somewhat below the calculated curve. Previous comparison of Eq. (1) with data for noncavitating hydrofoil sections with a rounded leading edge indicated generally satisfactory agreement (Figs. 3 to 8). The theoretical curves based on Eq. (1) in Figs. 13c and 13d were taken from Ref. [2], as the Froude number for these conditions was larger than those used in computations carried out at this Laboratory. Only three points at $x/c = 15$, 20, and 25 could be obtained from the cross plots in Ref. [2], although these are sufficient for the present purposes. There appears to be very little variation in the downwash angle with cavitation number for the limited experimental data, particularly at the higher velocity. If the discrepancy between the theory and data for the fully wetted condition in Fig. 13a is neglected, the effect of the long trailing cavity is to increase the downwash angle over that for the fully wetted foil.

(2) <u>Two Foils Forward, One Aft</u>

Some measurements were also made with forced ventilated foils in another configuration. The configuration consisted of two foils forward and a single foil aft. The results of these tests are plotted in Figs. 14 and 15. The parameter, y, indicates the lateral spacing or split of the forward foils measured from the longitudinal centerline of the foil system, as shown in the definition sketch of Fig. 2. The experimental data for the lift and drag forces and cavitation numbers of the aft foil were reduced in terms of the same parameters as used in Figs. 11a to 11h and were plotted on a common graph for a given set of conditions. Note that the triangular symbols refer to cavitation number. In each of these figures, it will be noted that practically no interference effect exists when the initial cavities on the forward and aft foils are long. For the case where the aft cavity is shorter than the forward cavity, as shown on the plots at the right in Fig. 14, the forces and cavitation numbers have been reduced slightly. The exception to this trend is in Fig. 15, where for all practical purposes no interference effect on the force coefficients exists for nearly all foil separations in the longitudinal direction.

To relieve some of the difficulties experienced with forced-ventilated foils, a series of tests was conducted with naturally ventilated foils forward and aft. These foils were ventilated to the atmosphere by means of a parabolic base vented strut; thus the cavitation number was a function of the foil submergence and velocity. The cavity pressure was assumed to be essentially atmospheric and therefore constant. The results of these tests are shown in Figs. 16, 17, and 18 for various longitudinal and lateral foil separations and various flow conditions. In each of these figures, the value of the cavitation number given applies to both the forward and aft foils and is assumed not to change with longitudinal separation of the foils, x/c. The experimental data shown in Fig. 16 for $y = 0$ were taken with one foil forward and one foil aft. It can be seen that for the higher σ (lower velocity) the force coefficients for the aft foil have generally been reduced by the interference effect for all longitudinal separations. For lower σ (higher velocity) the interference effect practically disappears except for small foil separations. At a higher angle of attack, the force coefficients are apparently not changed. This is somewhat surprising, as both the lift coefficient and the length of the cavity for the forward foil are greater at an angle of 18 degrees than at 14 degrees, other conditions being the same. It was expected that the downwash angle would increase with both lift coefficient and cavity size.

The interference effects for two forward foils split at lateral distances of two and four chords are shown in Figs. 17 and 18 respectively. In comparing the results for the zero and two chord foil separation, it can be seen that the force coefficients of the aft foil tended to increase slightly as the foils were split. This tendency disappeared at the higher angle of attack. With the forward foils split at four chords, the interference effect was negligible. A small oscillatory trend may be noted with longitudinal separation at the lower velocities. This may be caused by the wave patterns generated by the forward foils and struts converging in the vicinity of the aft foil.

Another type of interference was noted in the tests with the base vented struts. For some conditions, the cavity attached to the strut on the aft foil was modified by the wave pattern generated by the forward strut. The general effect was to disrupt the strut cavity to the extent that it could not be maintained over the length of the test run. The strut cavity partially closed, which resulted in an increase in the cavitation number on the foil itself. As such a behavior was readily recognized by visual observation, these results were not included in the previous figures.

V. CONCLUSIONS

1. Experimental measurements were made of the interference effects for two submerged, noncavitating hydrofoils of aspect ratio 6 in a tandem configuration. Data for the average downwash angle as a function of velocity, submergence, and distance aft of the forward foil agreed satisfactorily with the theory of Ref. [1]. Particularly good agreement between the theory and experimental data was noted in the location of the maximum and minimum values of the downwash angle. Previous experiments [3] have shown that the variation of the downwash angle was closely associated with the surface wave generated by the foil.

2. The surface wave generated by a single, ventilated foil of finite span was measured for various velocities, angles of attack, submergences, and cavitation numbers. In general the disturbance was not as large as that for fully wetted foils, although relatively severe disturbances were found in the immediate vicinity of the trailing cavity. The wave amplitude increased with increasing cavitation number, primarily through an increase in lift coefficient, and decreased as the submergence of the foil was increased.

3. Tests with two fully submerged, forced-ventilated foils in a tandem configuration indicated that the total interference effect was dependent on the foil spacing and the initial cavitation numbers on the forward and aft foil. For long cavities (low cavitation numbers) a relatively small

change in the force characteristics of the aft foil was observed even though the cavity pressure for the aft foil changed considerably. For short cavities (higher cavitation numbers) a much greater variation in the force characteristics was found. In some cases, the cavity on the aft foil was lost due to interference effects. Similar trends were observed for naturally ventilated foils forward and aft.

4. For forced-ventilated foils, it appears that the ventilation characteristics of the aft foil may have been changed by interference from the forward foil. The surface wave from the forward foil had little effect on the aft foil compared to results previously obtained with noncavitating foils.

5. Measurements of the downwash angle for a forced-ventilated foil of aspect ratio 6, using a non-cavitating foil as a downwash meter, indicated that the downwash angle decreased monotonically with distance aft of the foil. For the limited data available, cavitation number had little influence on the non-dimensional downwash angle, ϵ/C_L.

6. With a configuration employing two foils forward and one foil aft, the interference effect was reduced to negligible values as the lateral spacing of the forward foils was increased. For some conditions with naturally ventilated foils, some difficulty was experienced in maintaining a well defined cavity on the parabolic, base vented strut.

ACKNOWLEDGEMENTS

The experimental data presented in the report are due to the efforts of many members of the Laboratory staff. The contributions of W. H. C. Maxwell, L. T. Boyer, and K. E. Foerster are to be especially acknowledged. F. R. Schiebe provided continual advice relative to the instrumentation problems. Preparation of the manuscript for printing was carried out by Kathleen Lagerberg, Patricia McNelly, and Marjorie Olson.

LIST OF REFERENCES

[1] Kaplan, P., Breslin, J. P., and Jacobs, W. R., Evaluation of the Theory for the Flow Pattern of a Hydrofoil of Finite Span, Stevens Institute of Technology, Experimental Towing Tank Report 561, May 1955.

[2] Yim, B., Downwash Due to a Fully Cavitated Hydrofoil Beneath a Free Surface, Hydronautics, Incorporated, Technical Report 001-12, July 1963.

[3] Wetzel, J. M. and Maxwell, W. H. C., Tandem Interference Effects of Flat Noncavitating Hydrofoils, University of Minnesota, St. Anthony Falls Hydraulic Laboratory, Project Report No. 61, May 1962.

[4] Maxwell, W. H. C., Interference Effects for Tandem Fully Submerged Flat Noncavitating Hydrofoils, University of Minnesota, St. Anthony Falls Hydraulic Laboratory, Memorandum No. M-92, March 1963. (Not available for distribution)

[5] Killen, John M., The Sonic Surface Wave Transducer, University of Minnesota, St. Anthony Falls Hydraulic Laboratory, Technical Paper No. 23, Series B, July 1959.

F I G U R E S

(1 through 18)

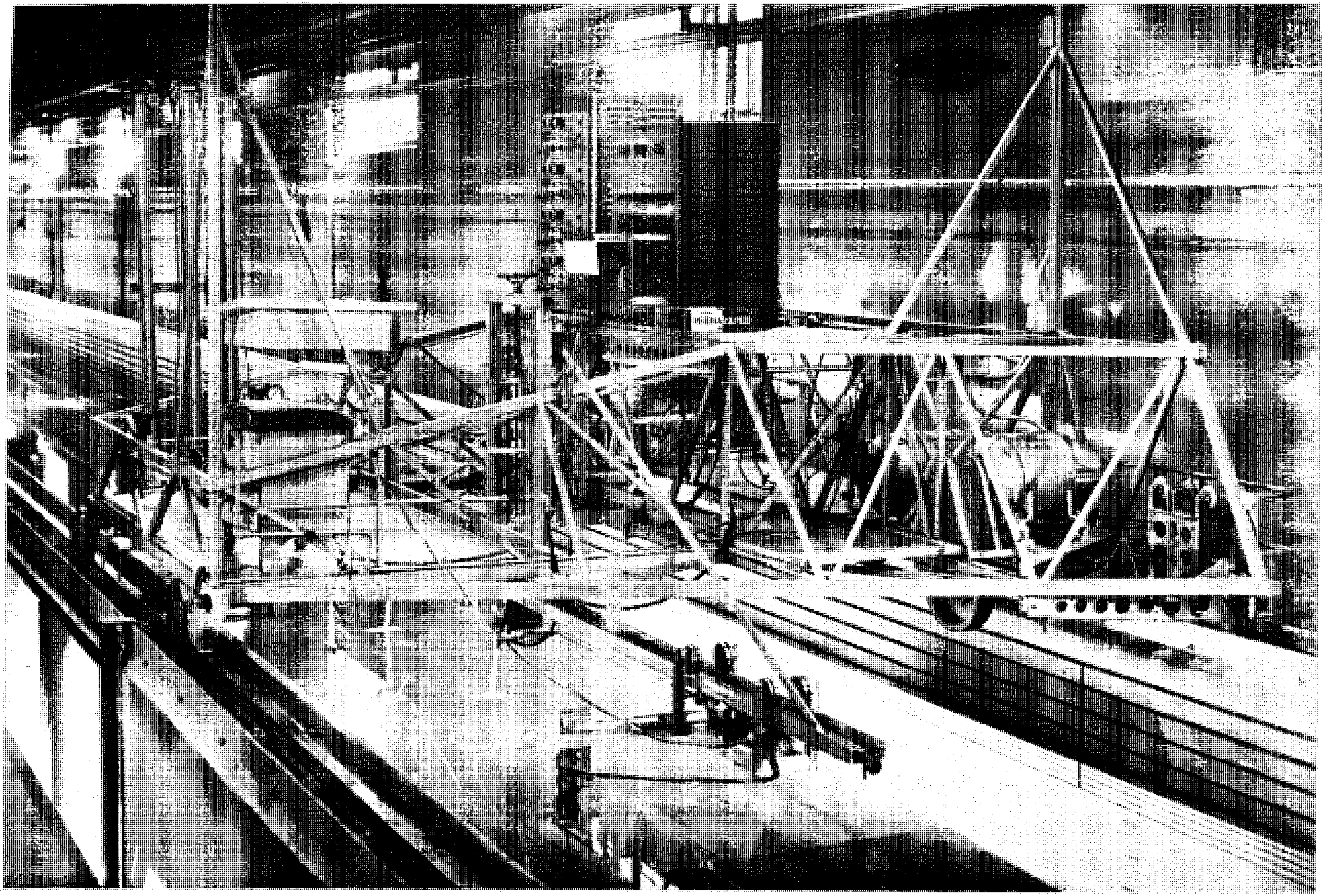

Fig. 1 - Photograph of Towing Carriage with Subcarriage used for Surface Wave Measurements

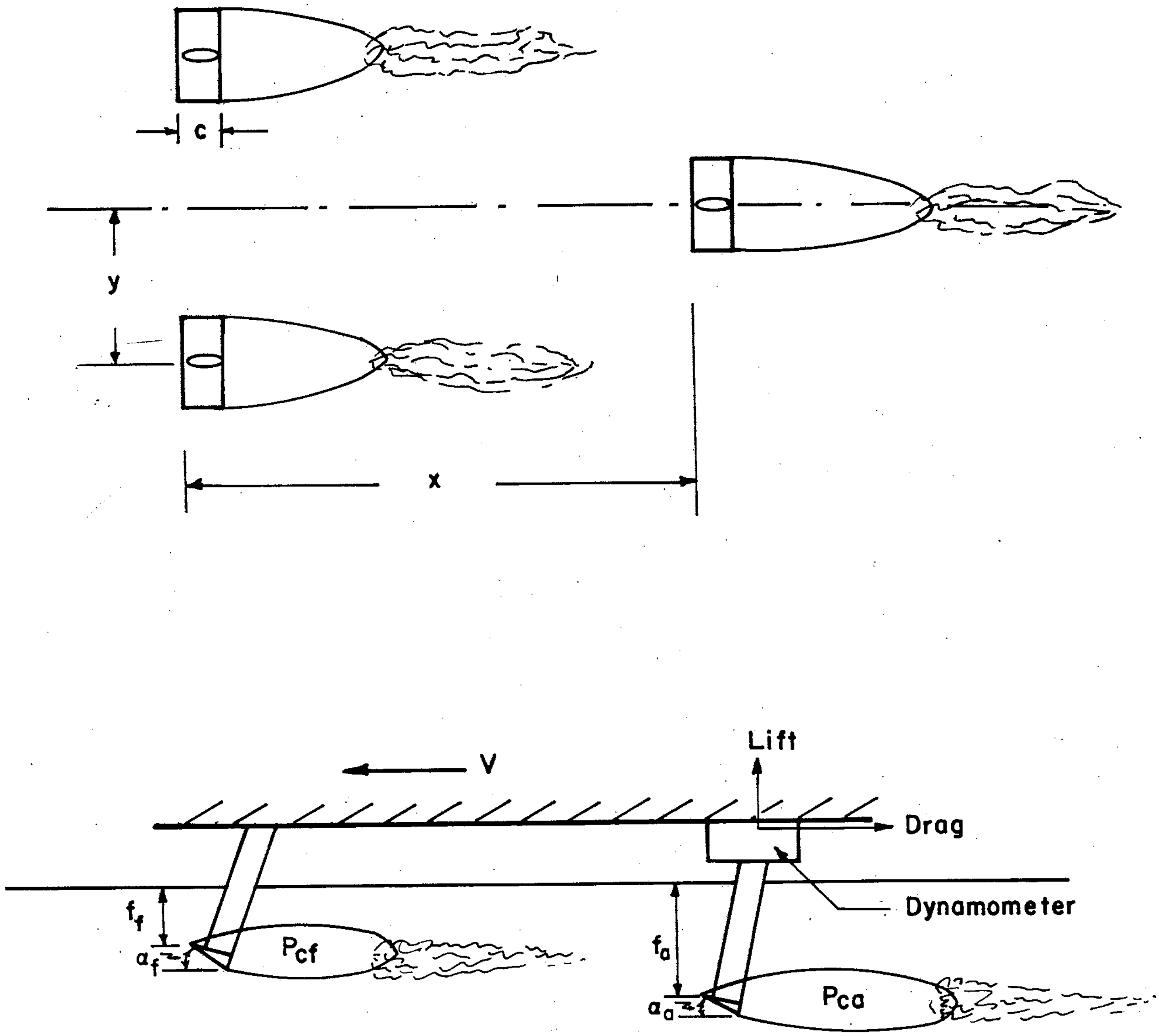

$$\sigma_f = \frac{P - P_{cf}}{\frac{1}{2}\rho V^2} \qquad \sigma_a = \frac{P - P_{ca}}{\frac{1}{2}\rho V^2}$$

Fig. 2 - Definition Sketch for Ventilated Foils

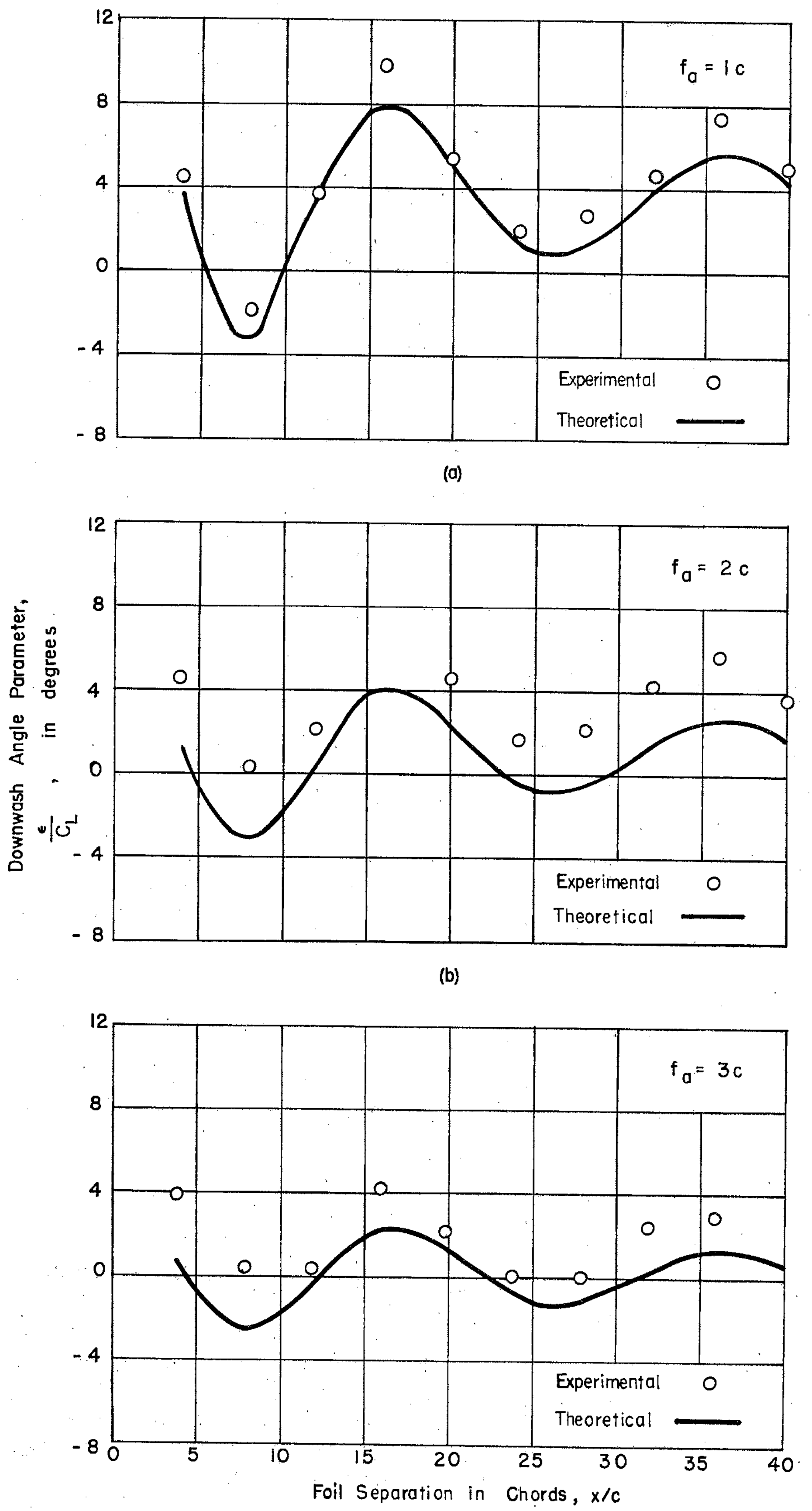

(c)

Fig. 3 - Variation of Downwash Angle with Foil Separation, Noncavitating Foil, AR = 6, f_f = 1c, V = 5 fps

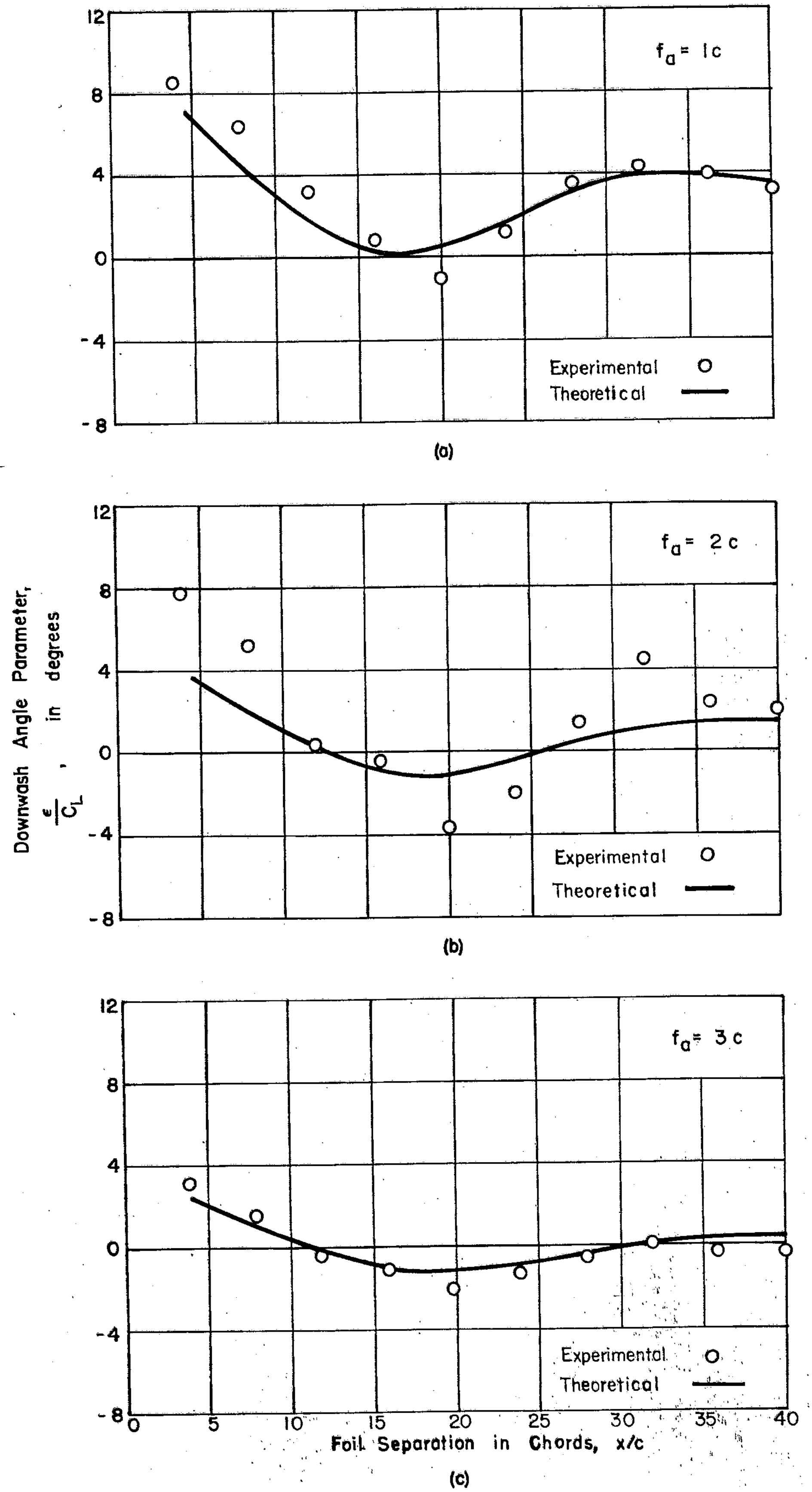

Fig. 4 - Variation of Downwash Angle with Foil Separation, Noncavitating Foil, AR = 6, f_f = 1c, V = 10 fps

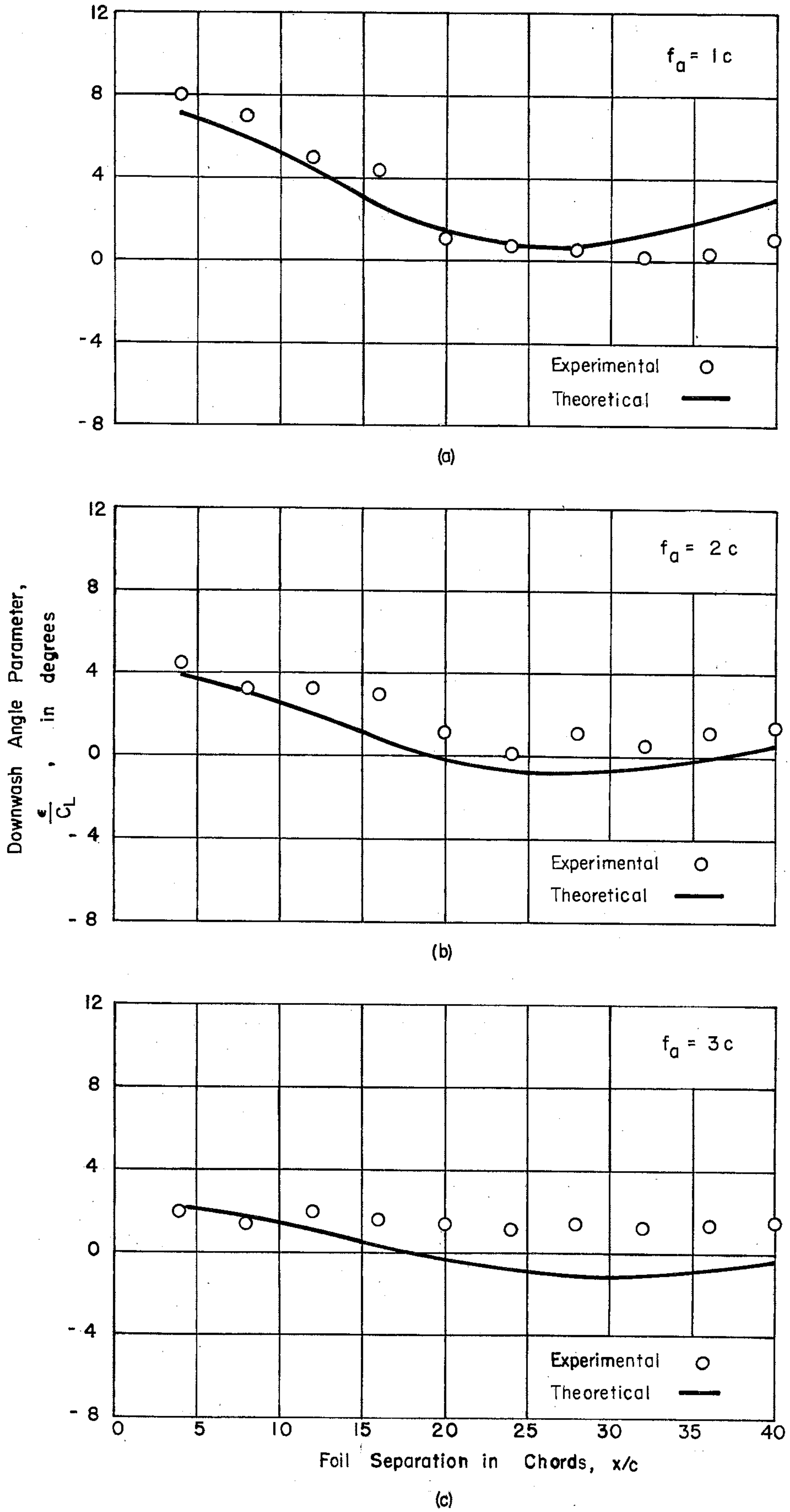

Fig. 5 – Variation of Downwash Angle with Foil Separation, Noncavitating Foil, $AR = 6$, $f_f = 1c$, $V = 15$ fps

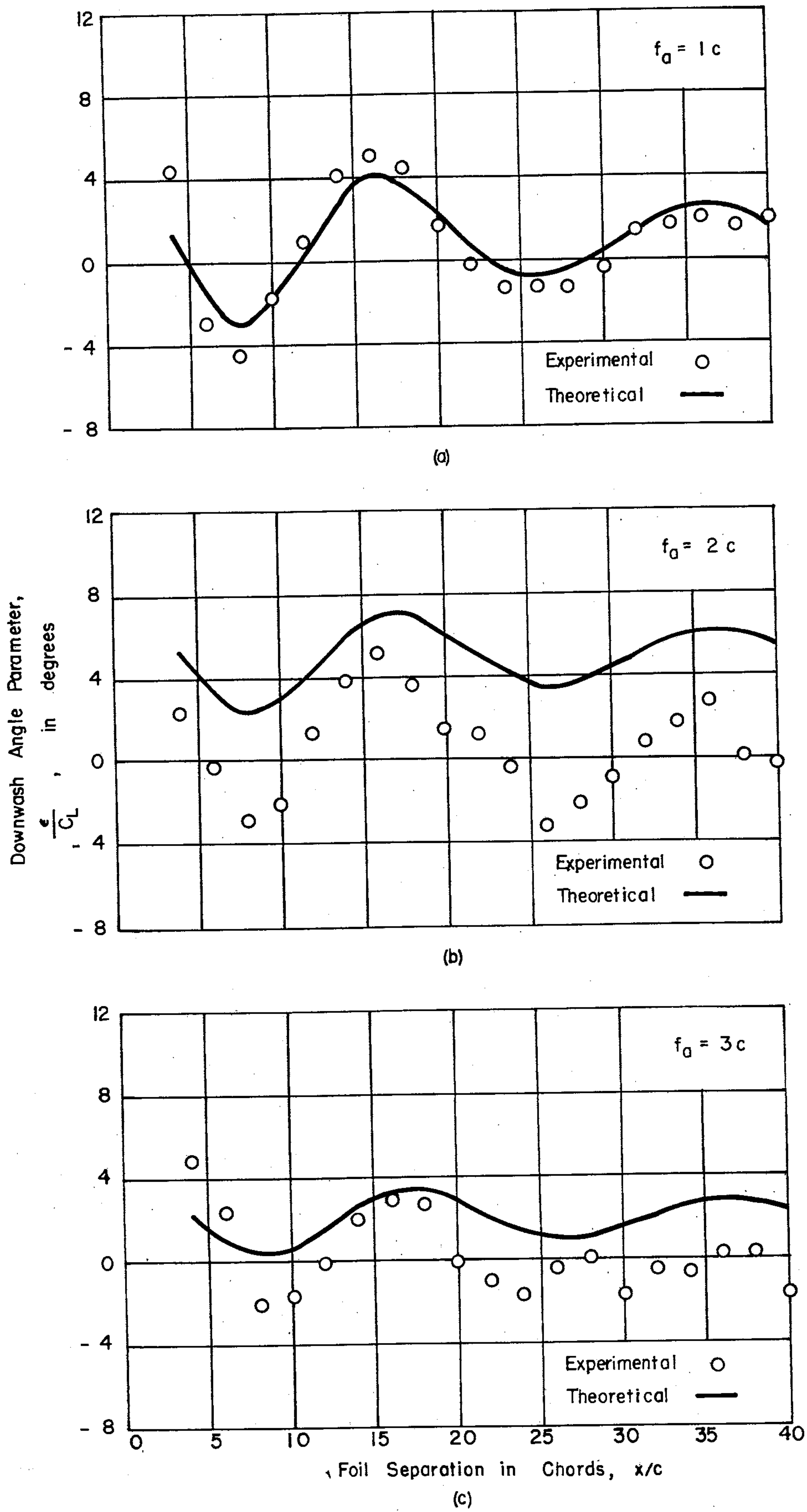

Fig. 6 - Variation of Downwash Angle with Foil Separation, Noncavitating Foil, AR = 6, f_f = 2c, V = 5 fps

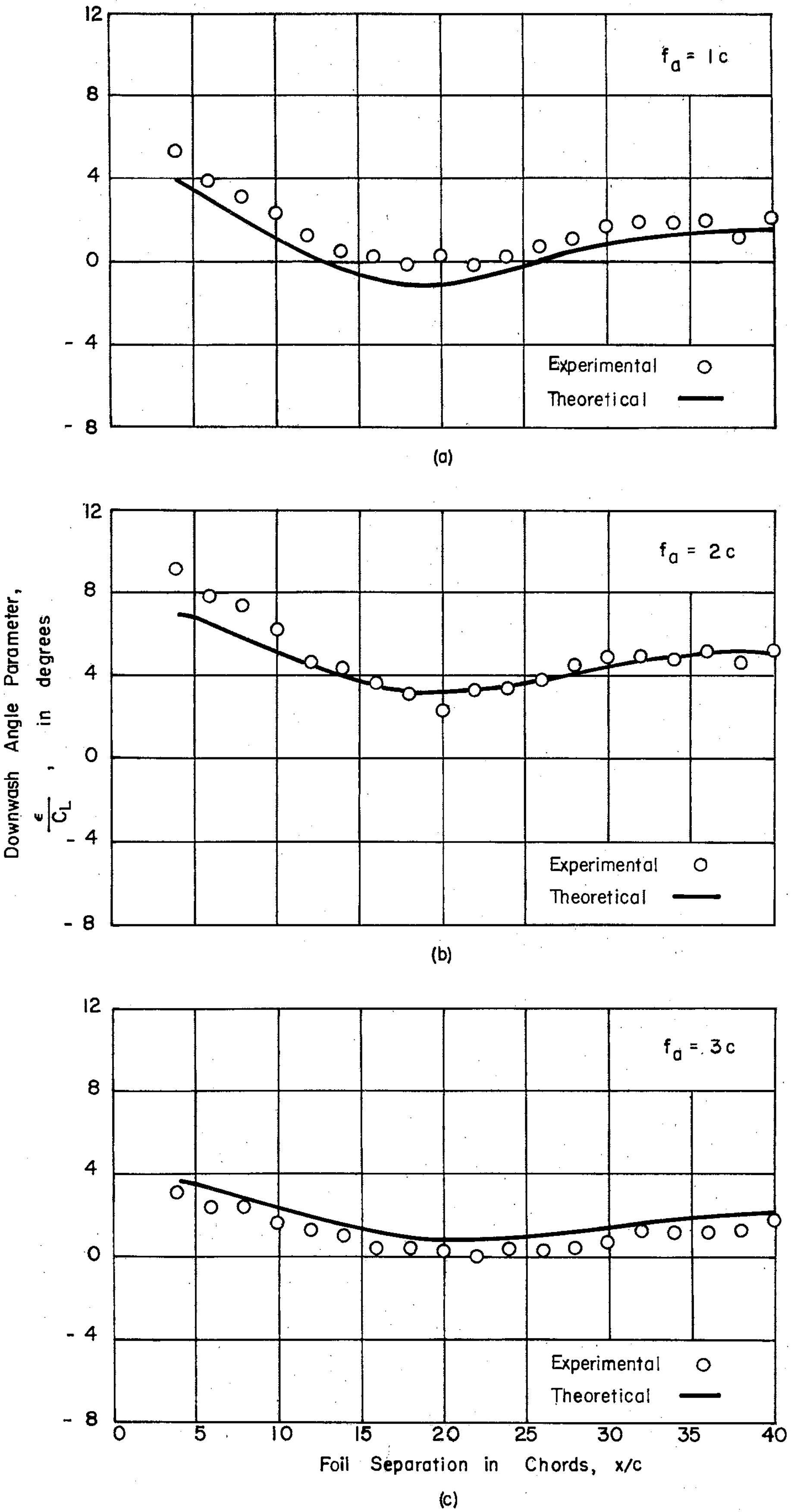

Fig. 7 - Variation of Downwash Angle with Foil Separation, Noncavitating Foil, AR = 6, $f_f = 2c$, V = 10 fps

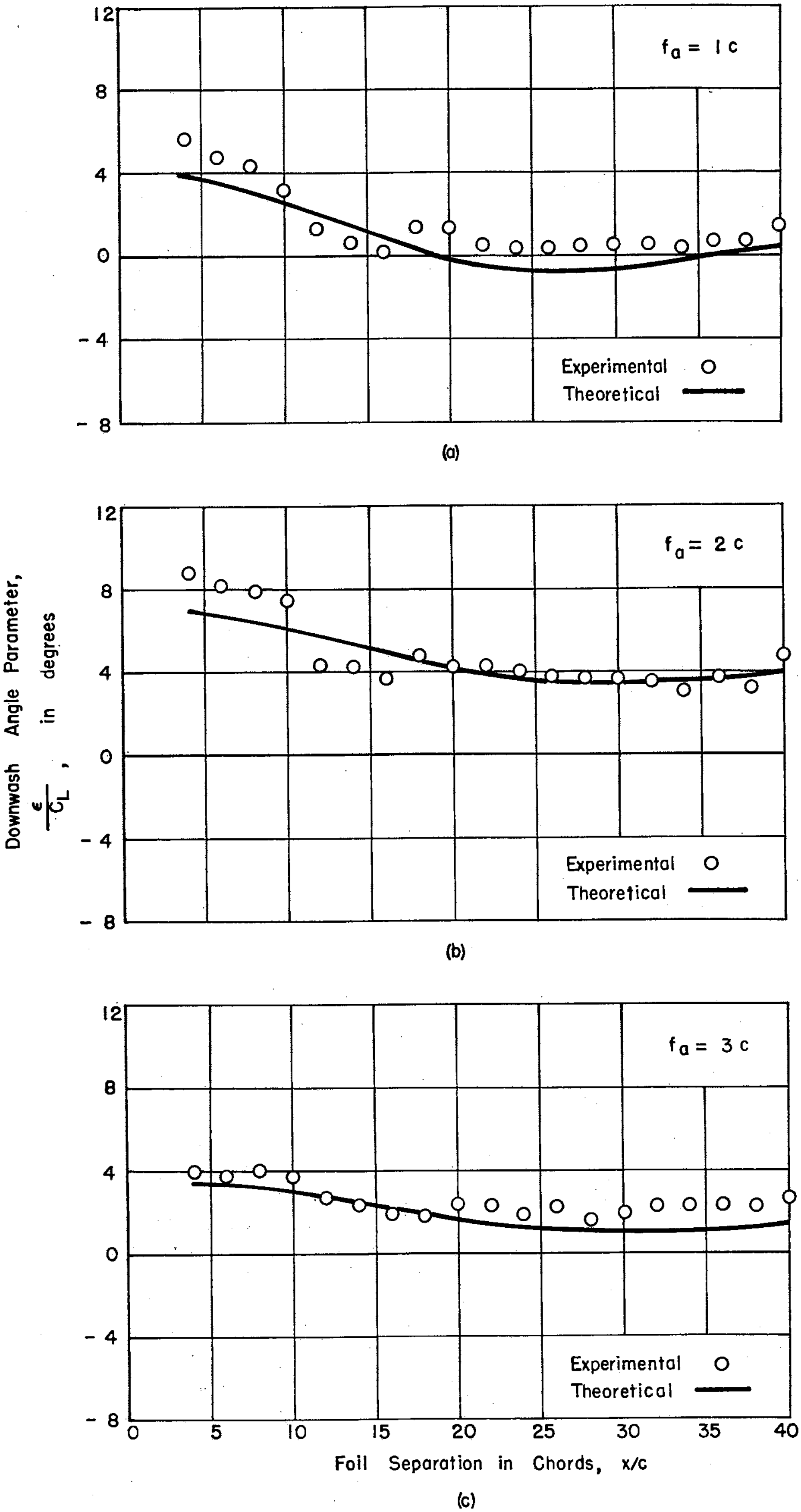

Fig. 8 - Variation of Downwash Angle with Foil Separation, Noncavitating Foil, AR = 6, f_f = 2c, V = 15 fps

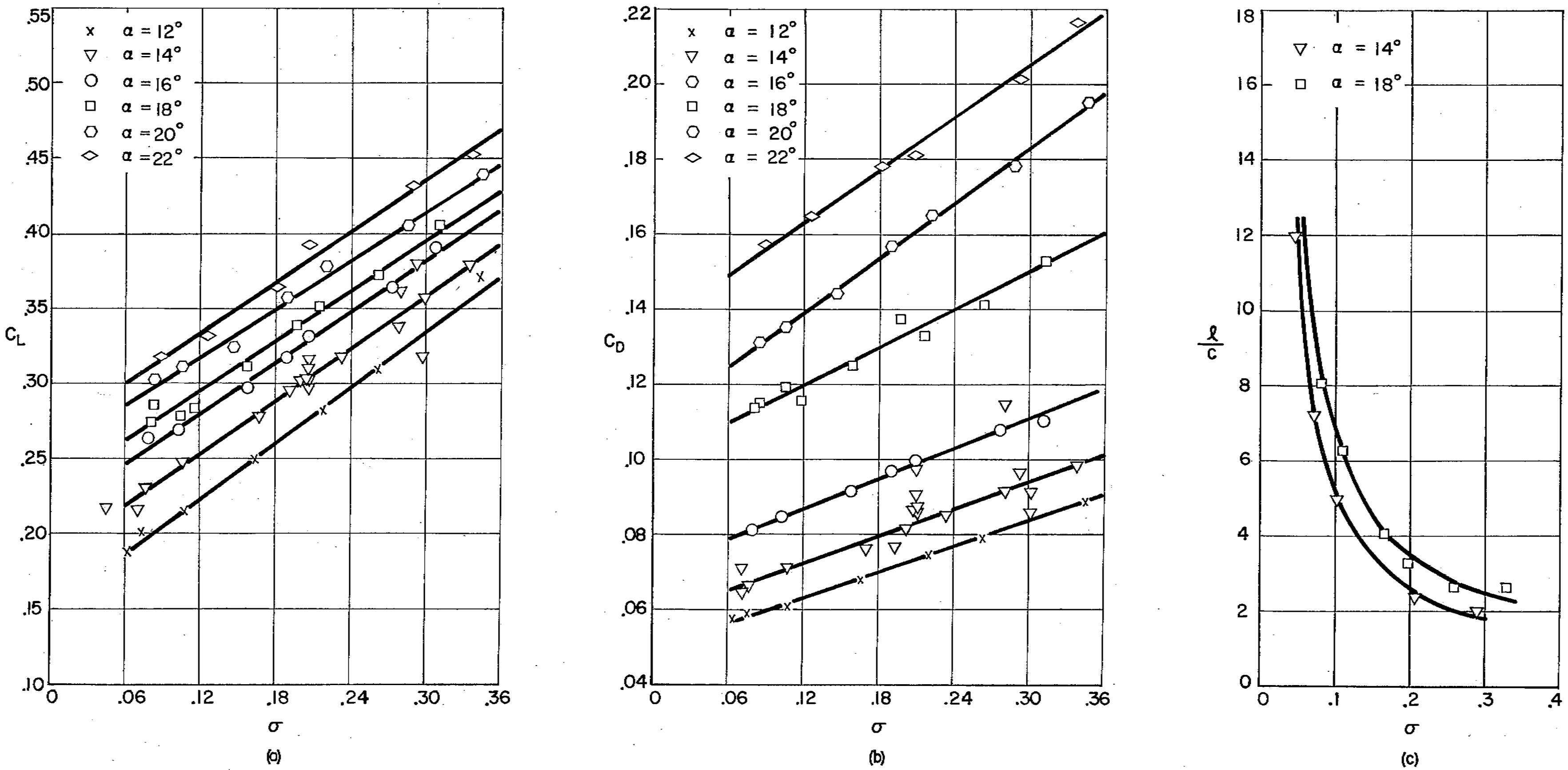

Fig. 9 - Force and Cavity Characteristics for Ventilated Foil, AR = 2, f = 1c

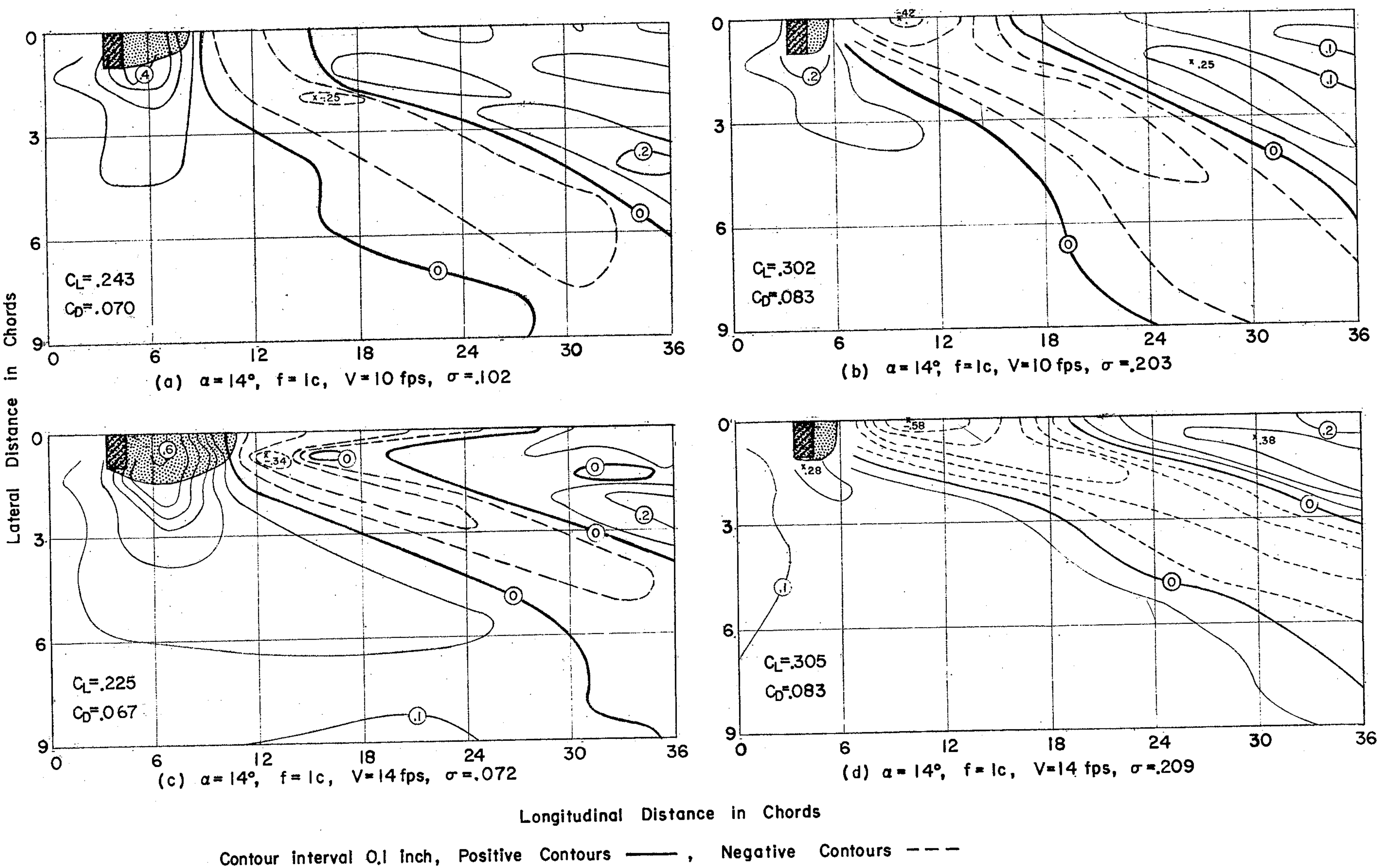

Fig. 10a, b, c, d - Surface Wave Contours for Ventilated Foil, AR = 2

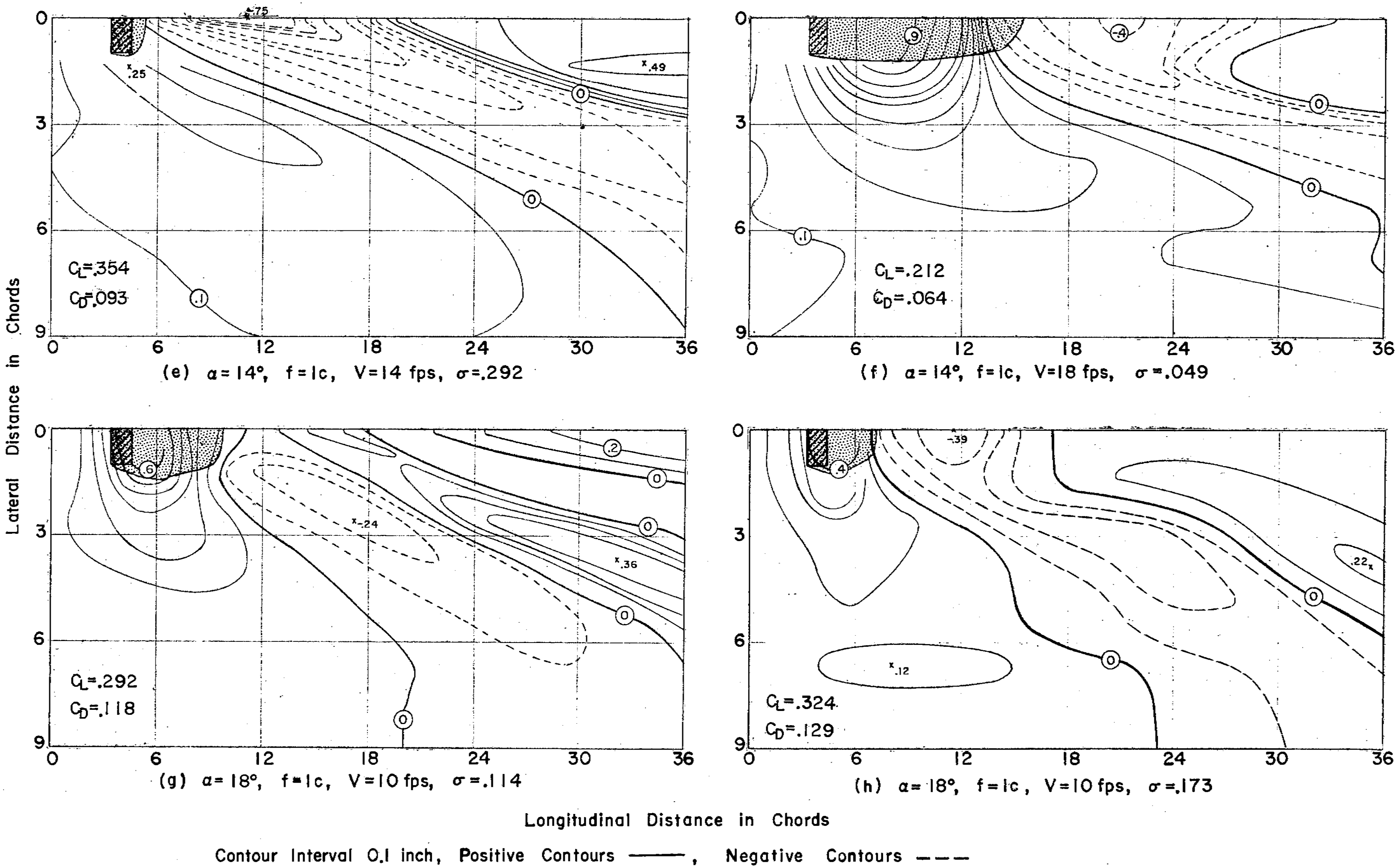

Fig. 10e, f, g, h - Surface Wave Contours for Ventilated Foil, AR = 2

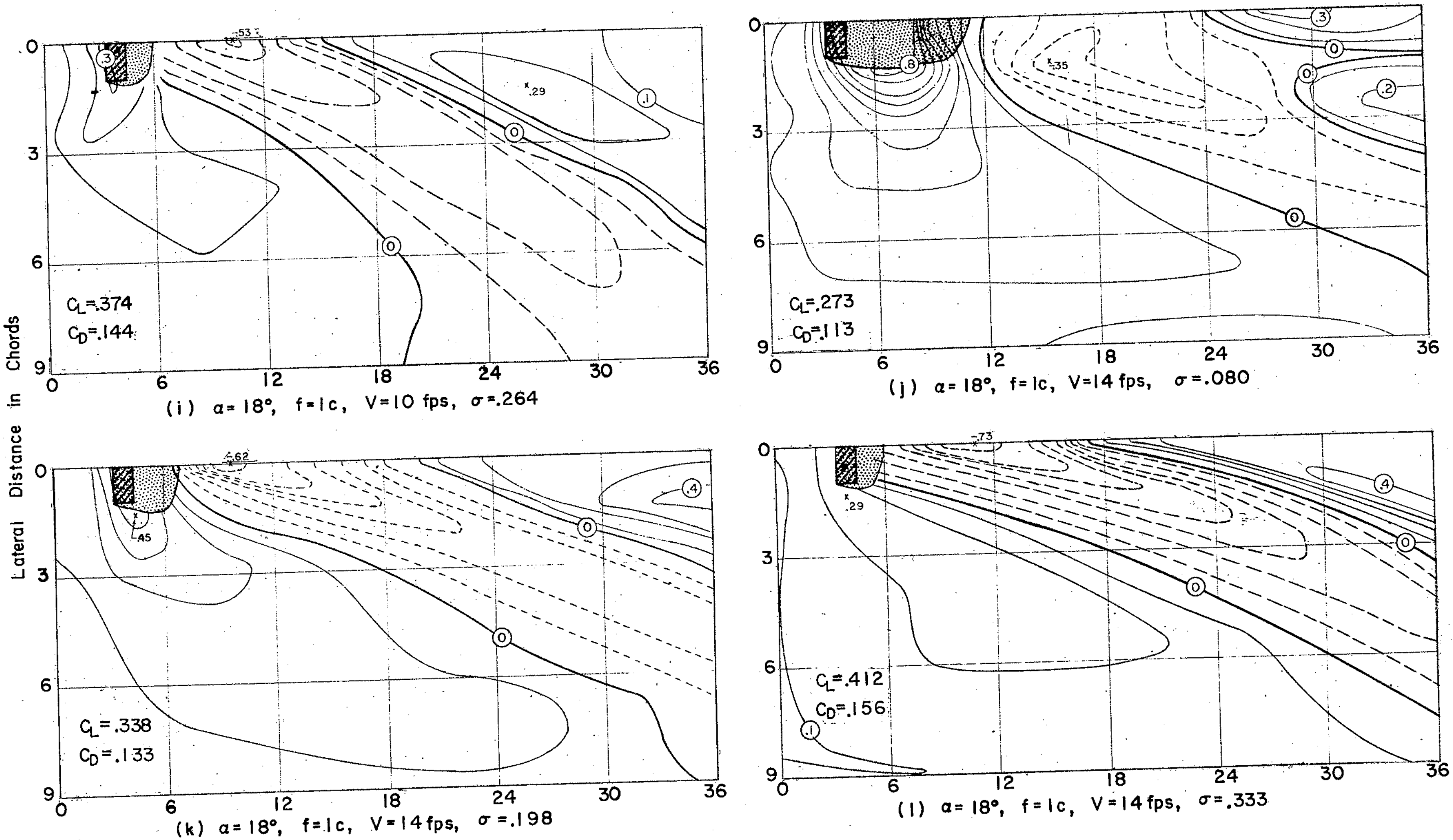

Longitudinal Distance in Chords

Contour Interval 0.1 inch, Positive Contours ———, Negative Contours - - -

Fig. 10i, j, k, l - Surface Wave Contours for Ventilated Foil, AR = 2

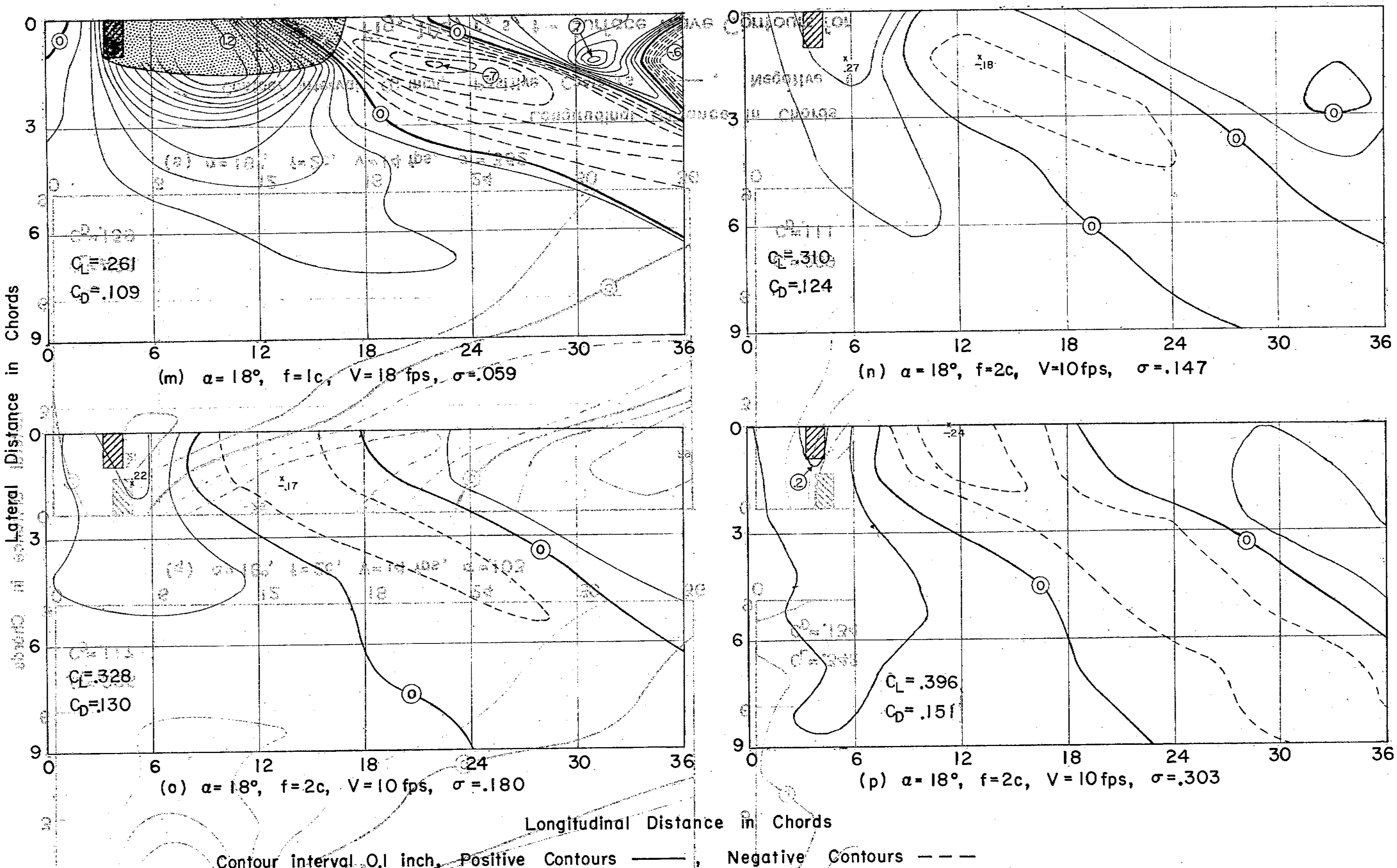

Fig. 10m, n, o, p - Surface Wave Contours for Ventilated Foil, AR = 2

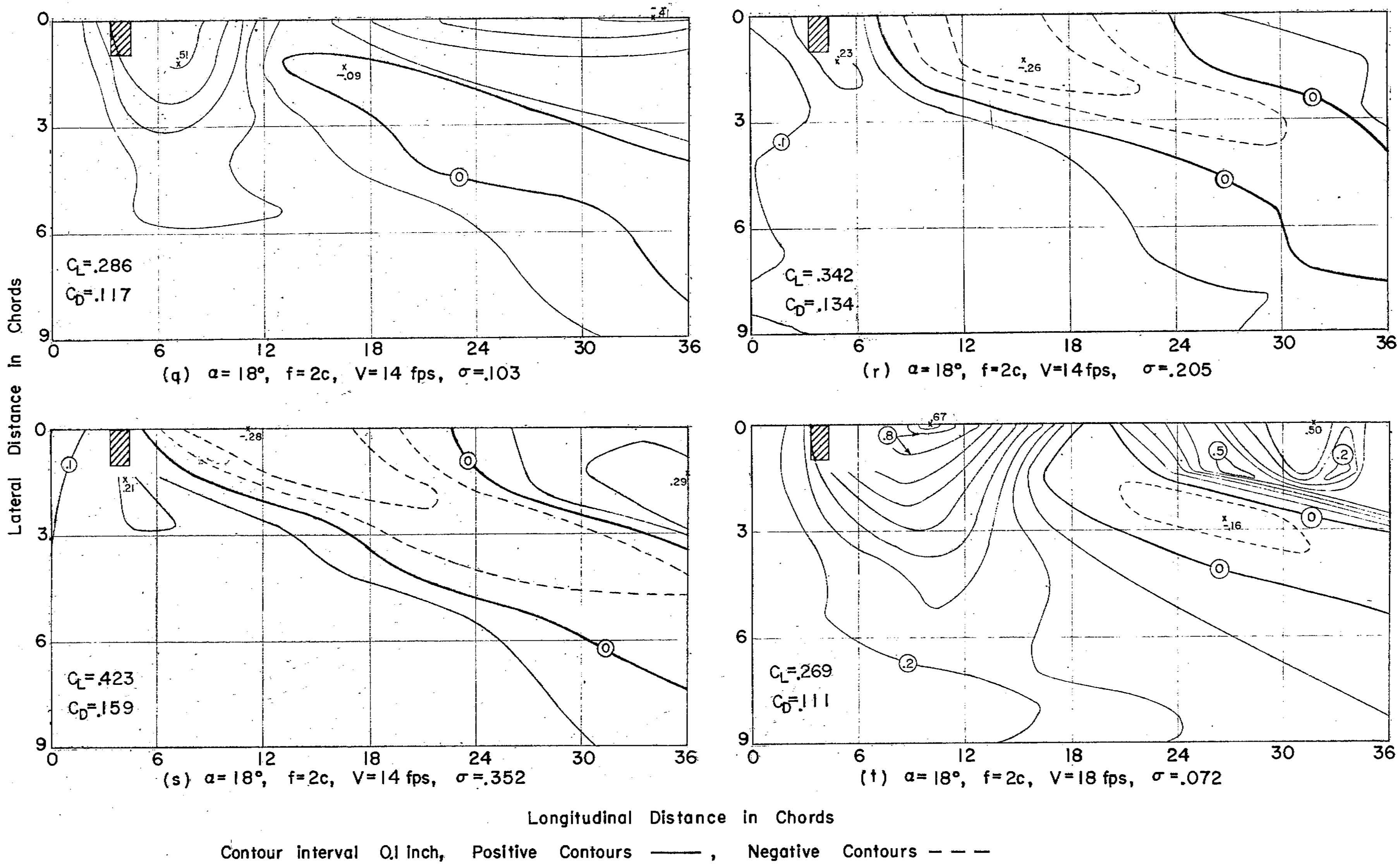

Fig. 10q, r, s, t - Surface Wave Contours for Ventilated Foil, AR = 2

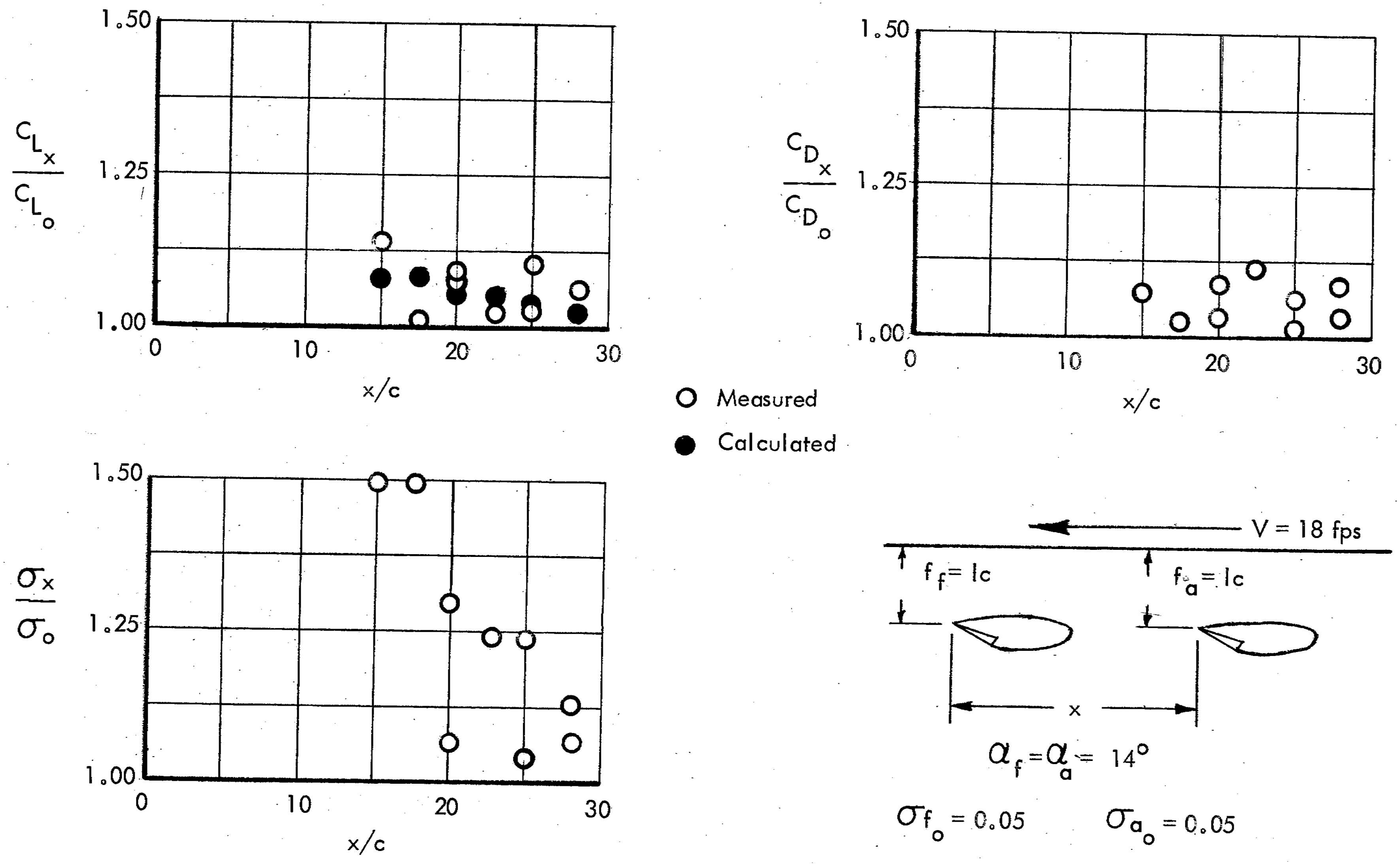

Fig. 11a - Tandem Interference Effects for Forced-Ventilated Foils, AR = 2, y = 0

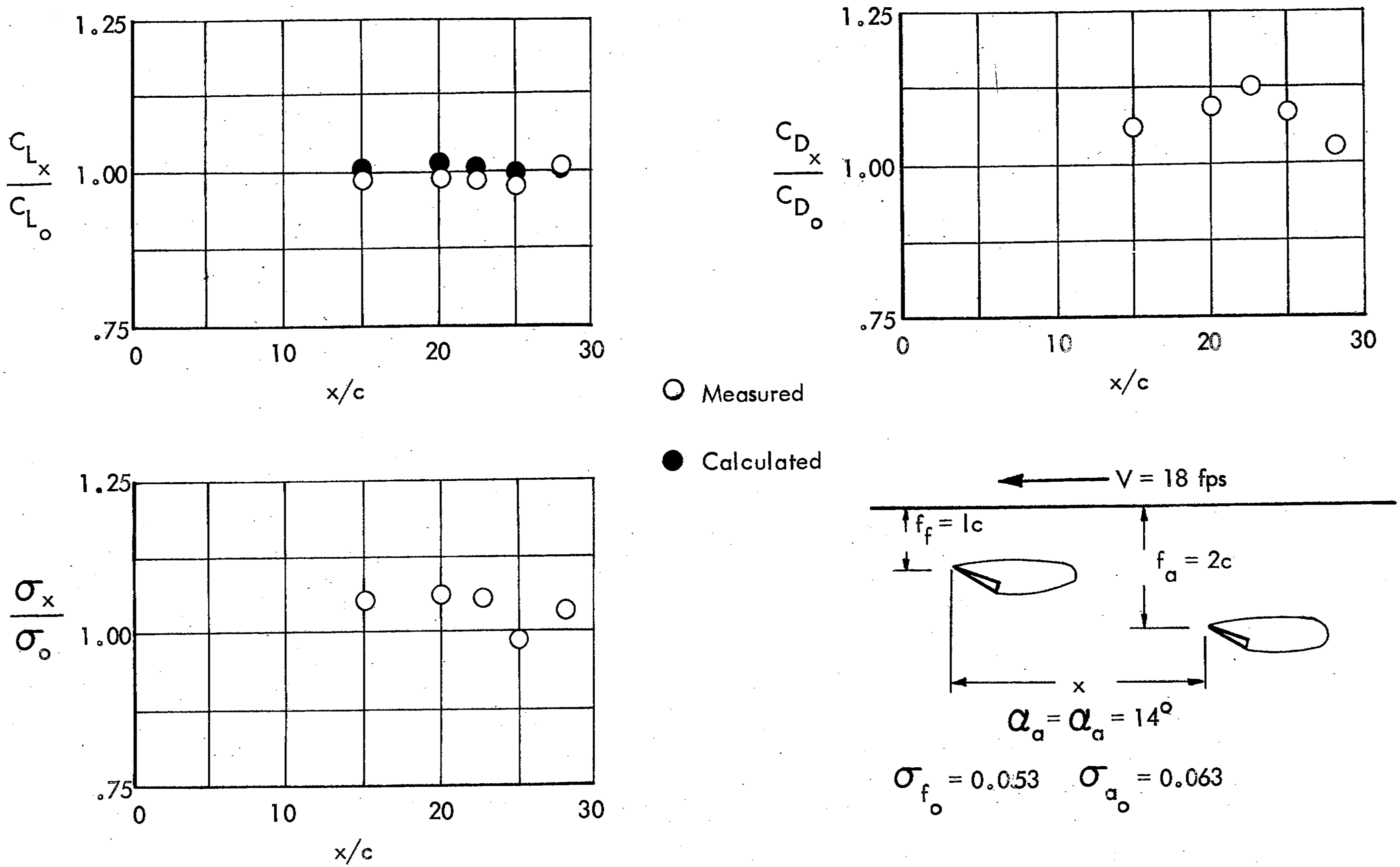

Fig. 11b - Tandem Interference Effects for Forced-Ventilated Foils, AR = 2, y = 0

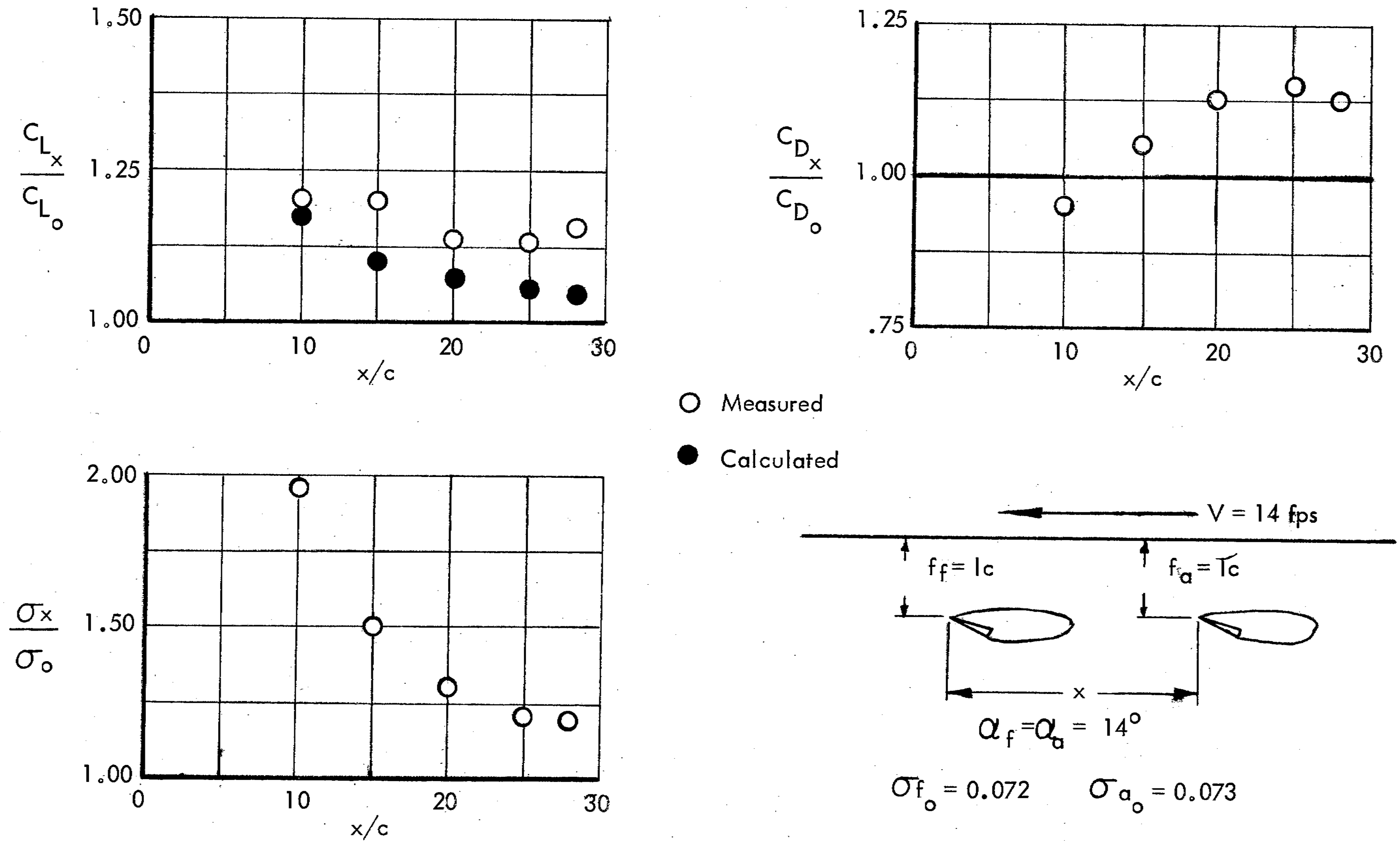

Fig. 11c - Tandem Interference Effects for Forced-Ventilated Foils, AR = 2, y = 0

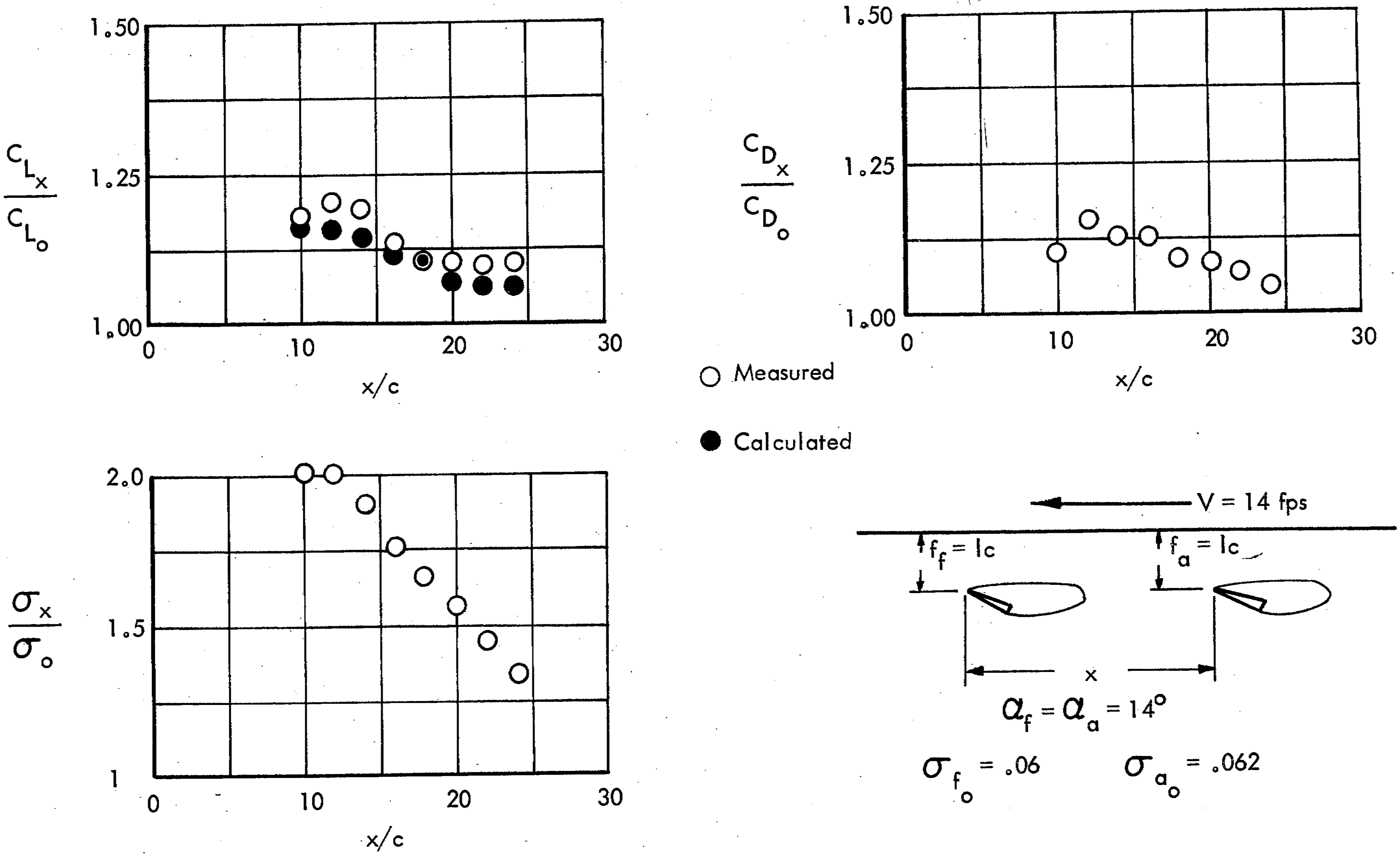

Fig. 11d - Tandem Interference Effects for Forced-Ventilated Foils, AR = 2, y = 0

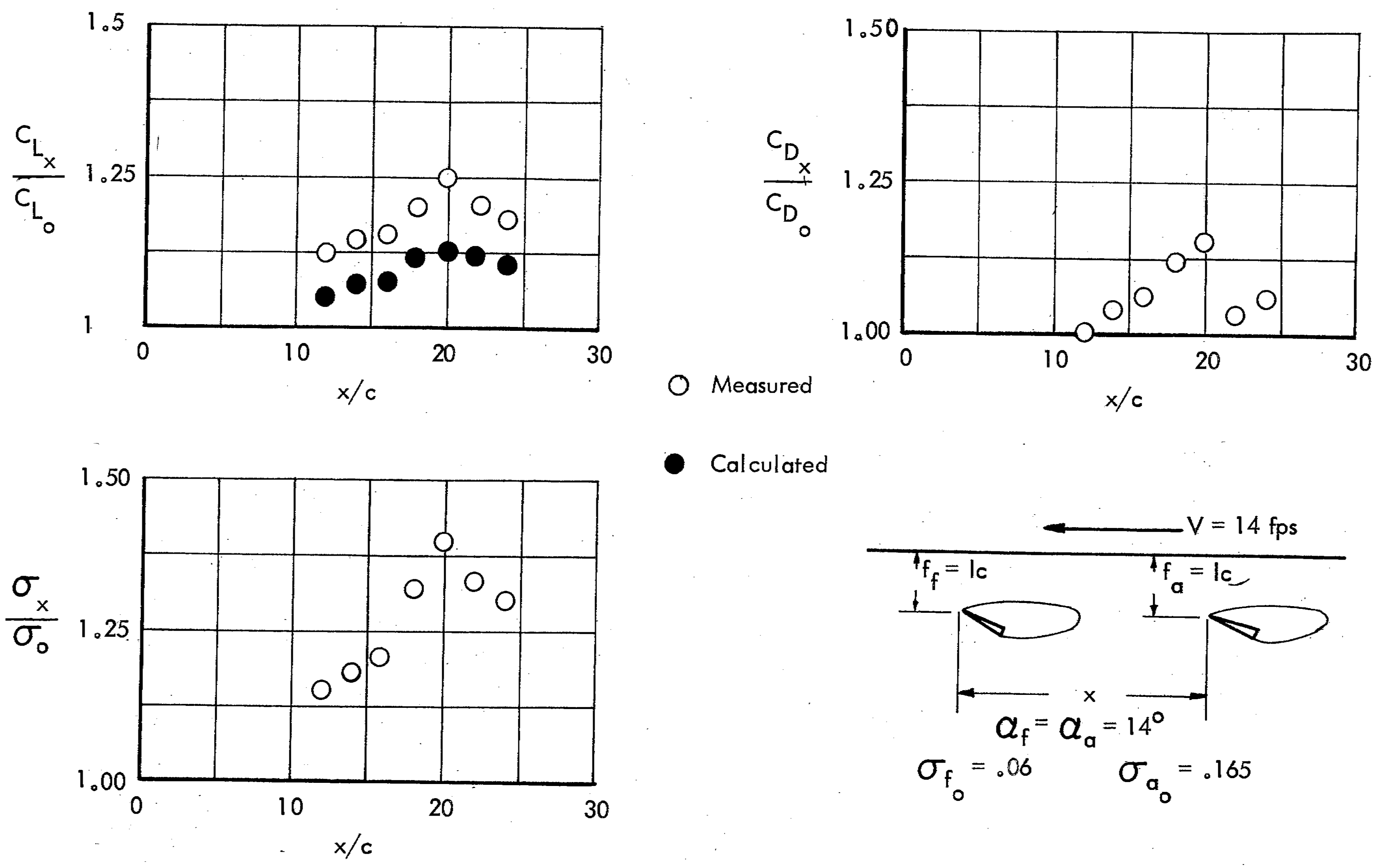

Fig. 11e - Tandem Interference Effects for Forced-Ventilated Foils, AR = 2, y = 0

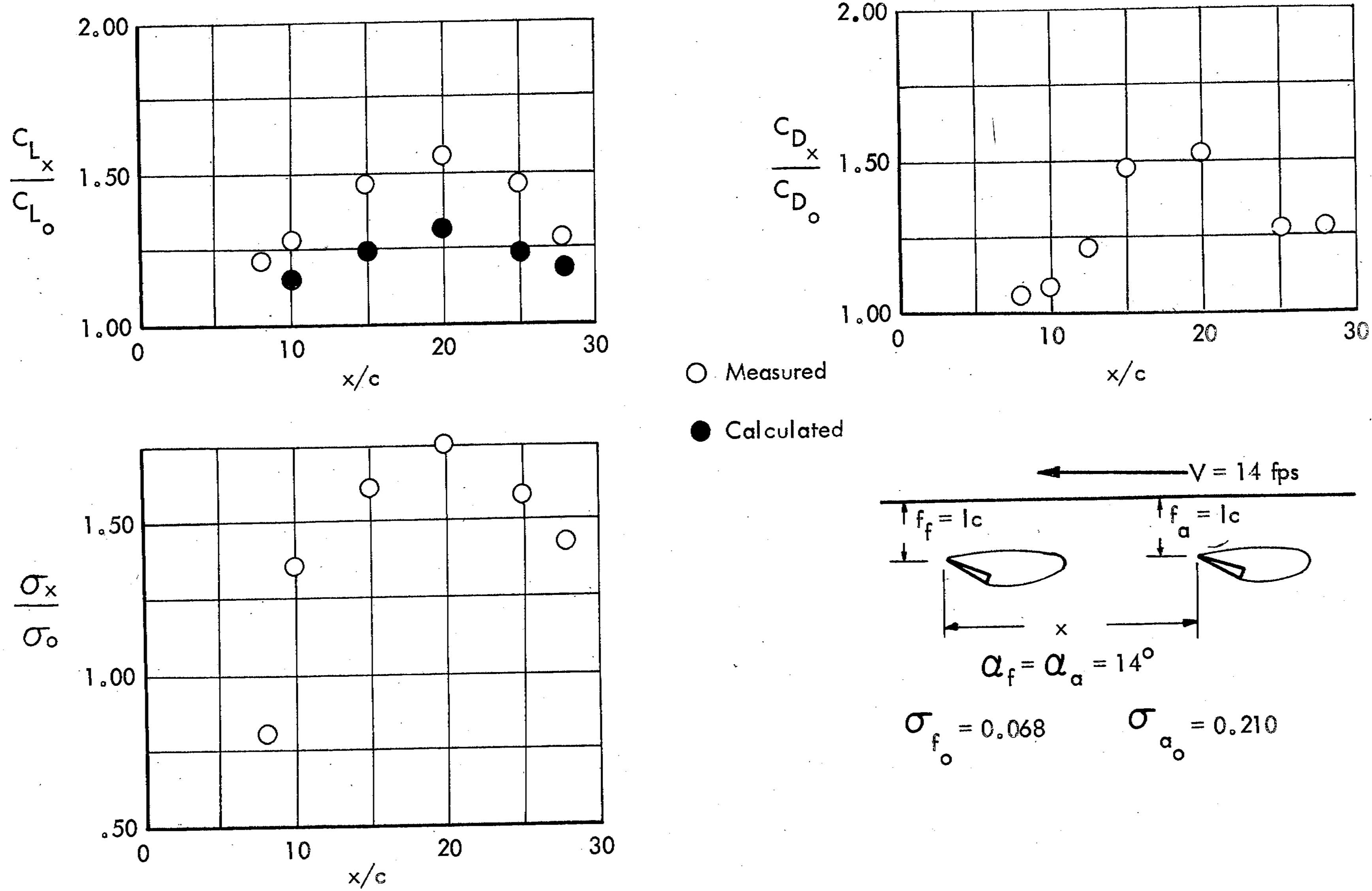

Fig. 11f - Tandem Interference Effects for Forced-Ventilated Foils, AR = 2, y = 0

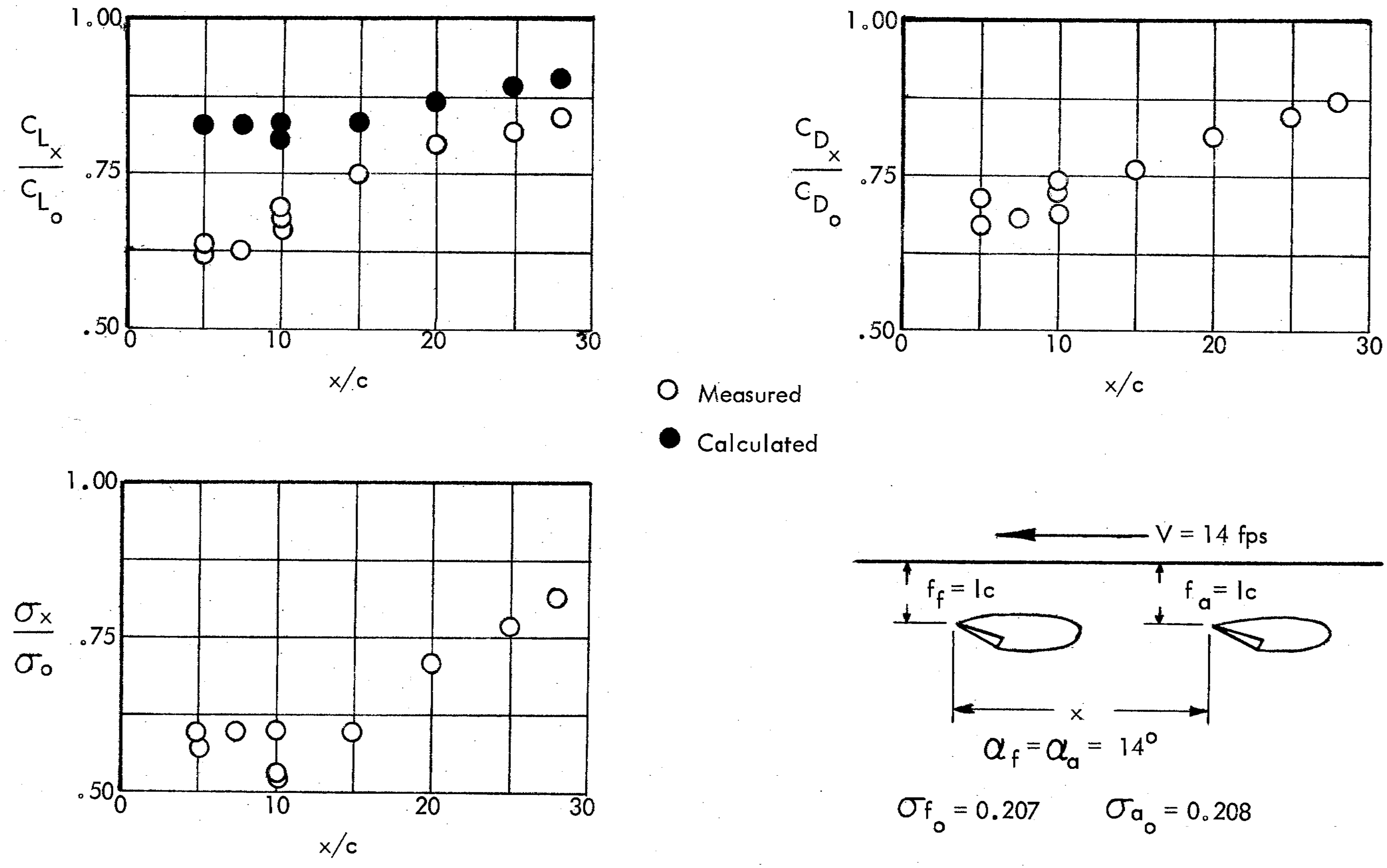

Fig. 11g - Tandem Interference Effects for Forced-Ventilated Foils, AR = 2, y = 0

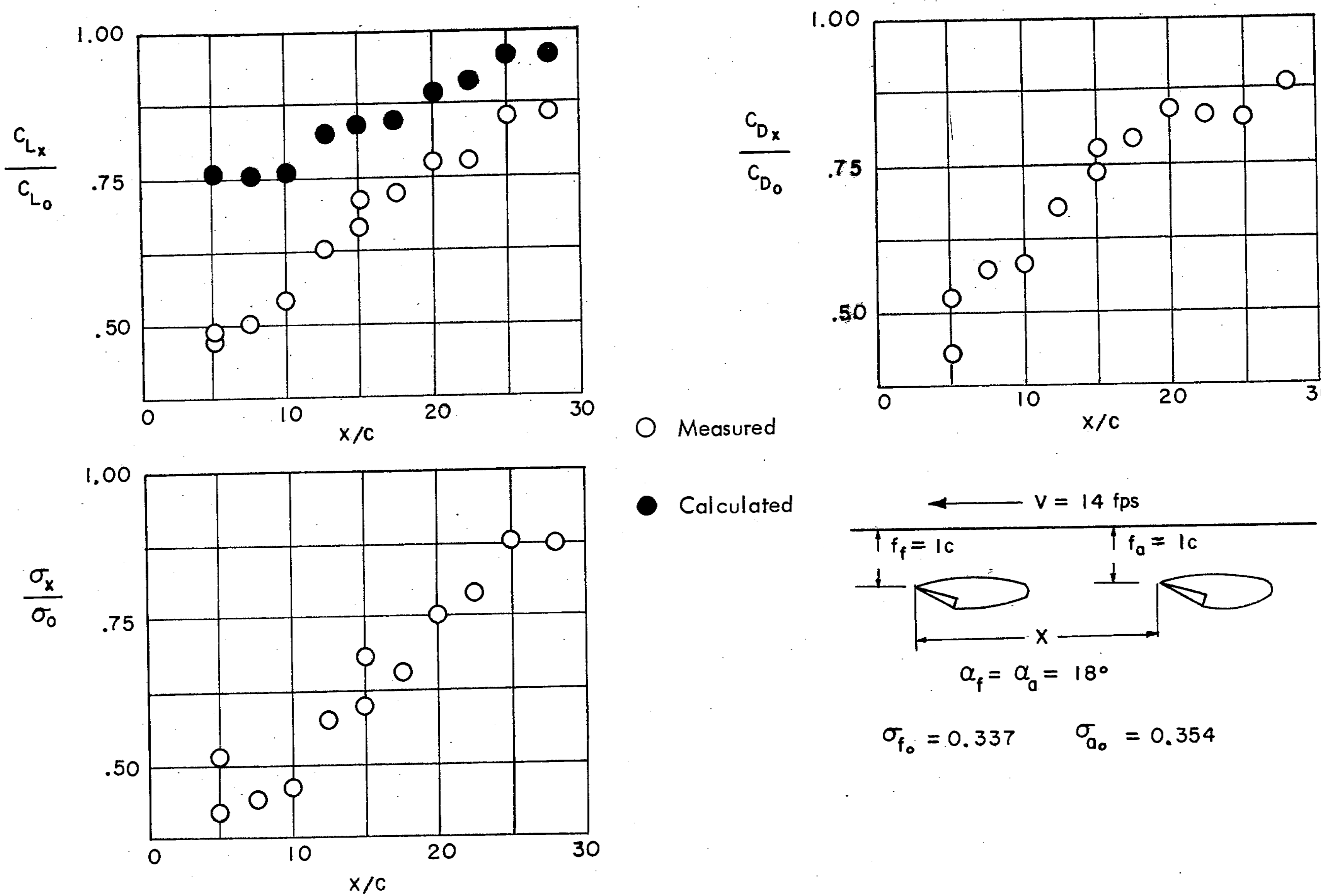

Fig. 11h - Tandem Interference Effects for Forced-Ventilated Foils, AR = 2, y = 0

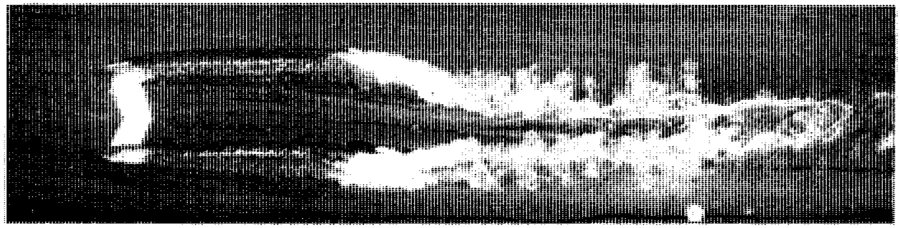

(a) $\sigma_f = 0.085$, $x/c = \infty$

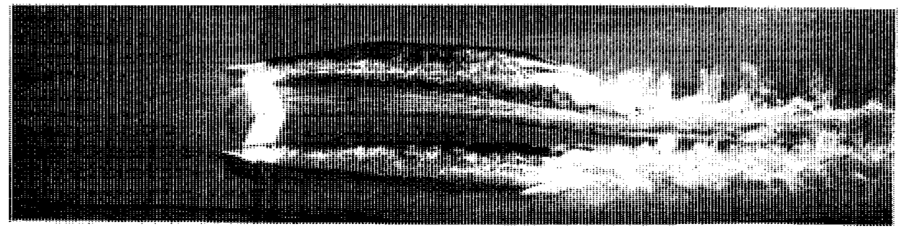

(b) $\sigma_a = 0.080$, $x/c = \infty$

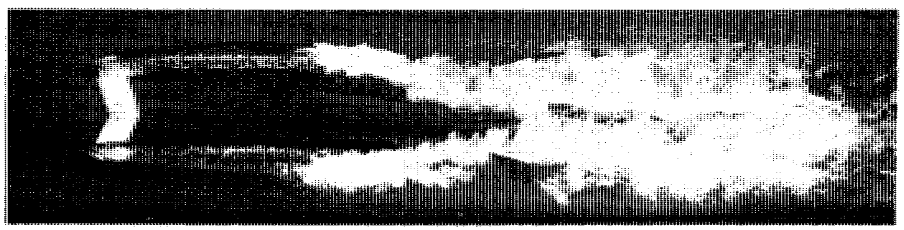

(c) $\sigma_a = 0.149$, $x/c = 10$

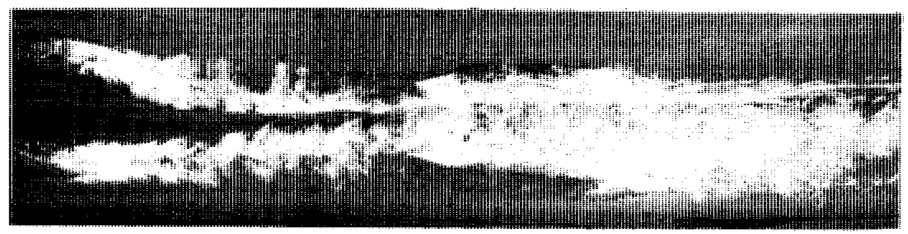

(d) $\sigma_a = 0.128$, $x/c = 15$

Fig. 12 - Photograph of Tandem Interference for Forced-Ventilated Foils

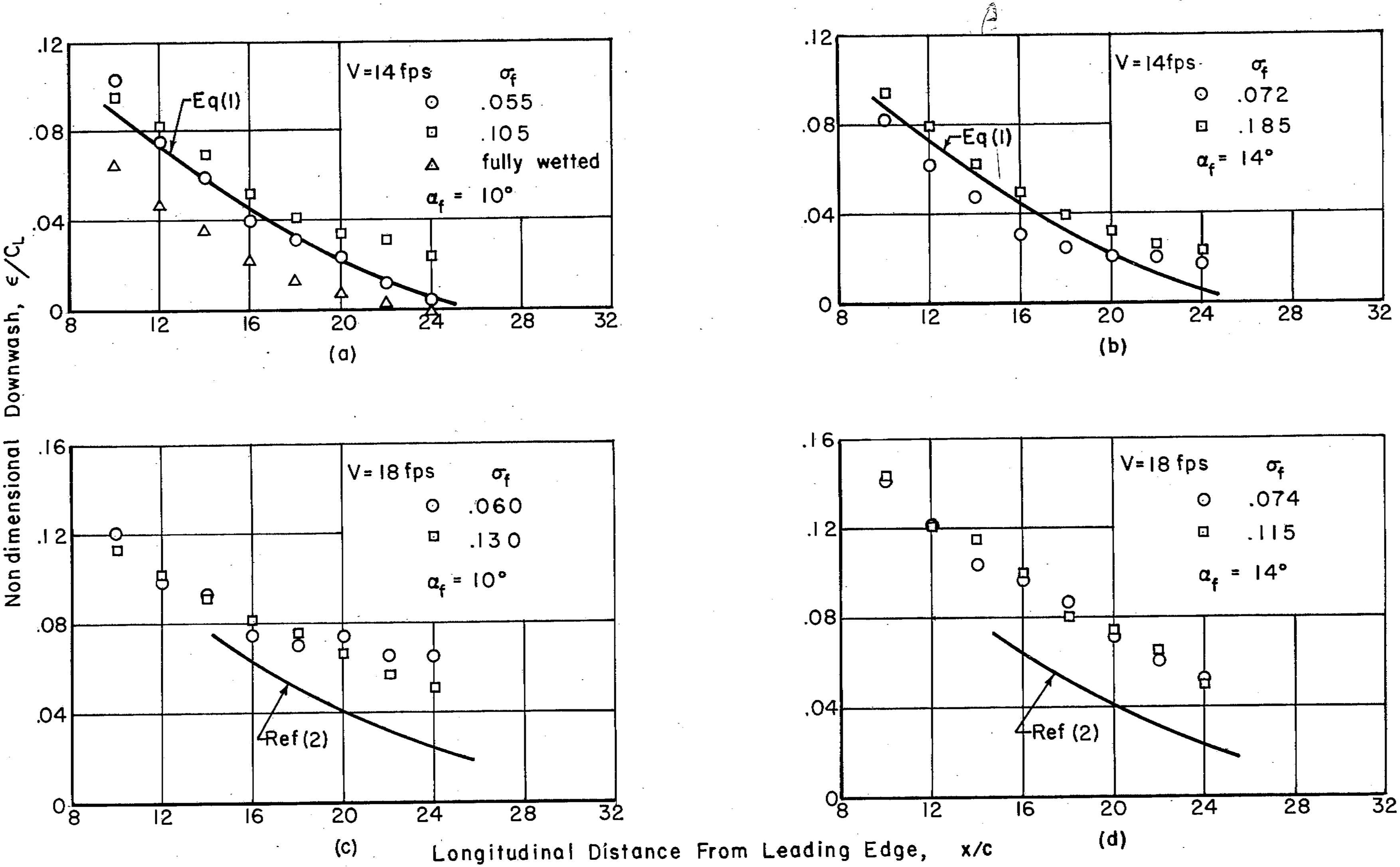

Fig. 13 - Average Downwash Angle for Forced-Ventilated Foil, AR = 6

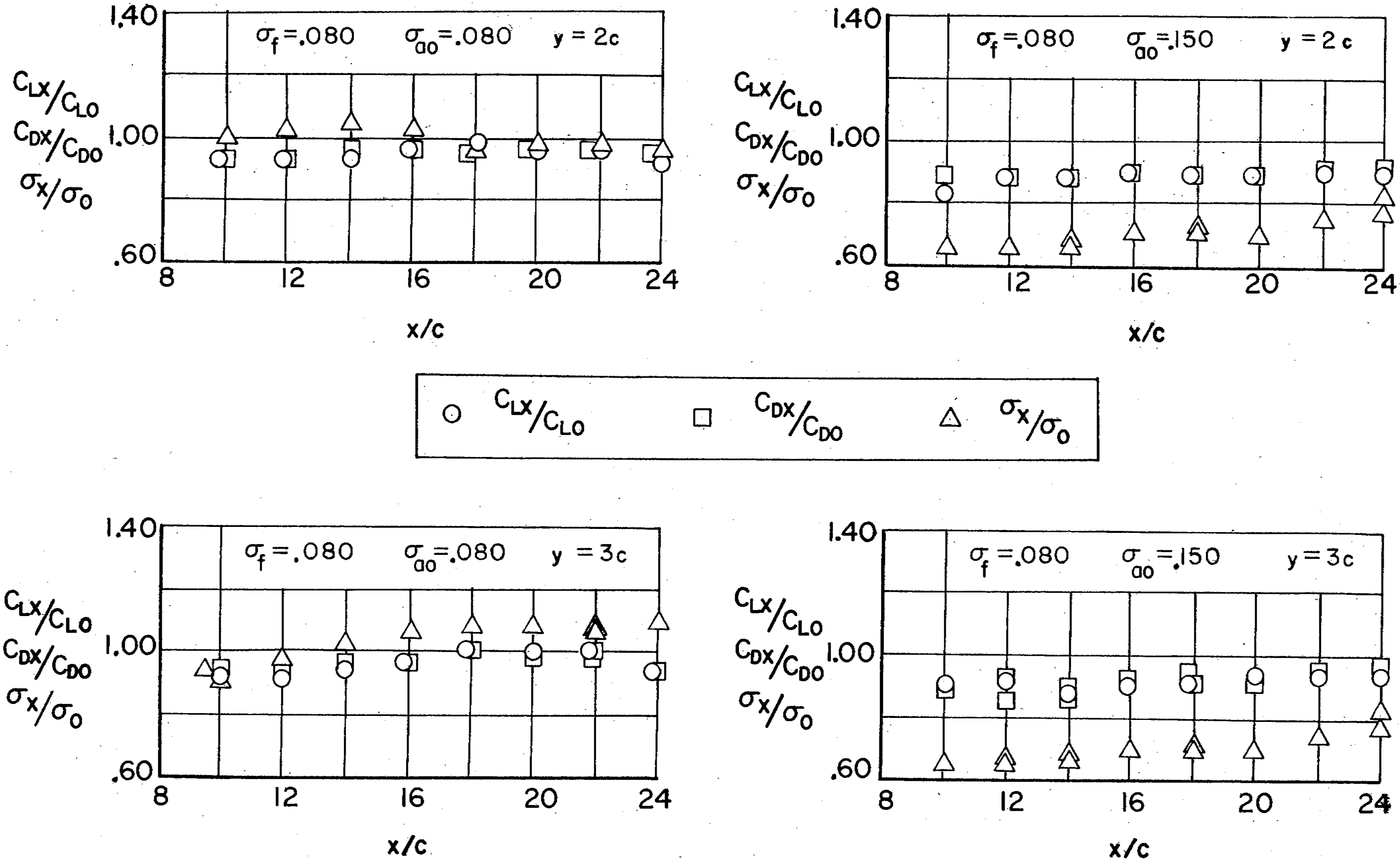

Fig. 14 - Interference Effects for Split Forward Foil System, Forced-Ventilated Foils,
$\alpha = 14^\circ$, $f = 1c$, $V = 12$ fps, $AR = 2$

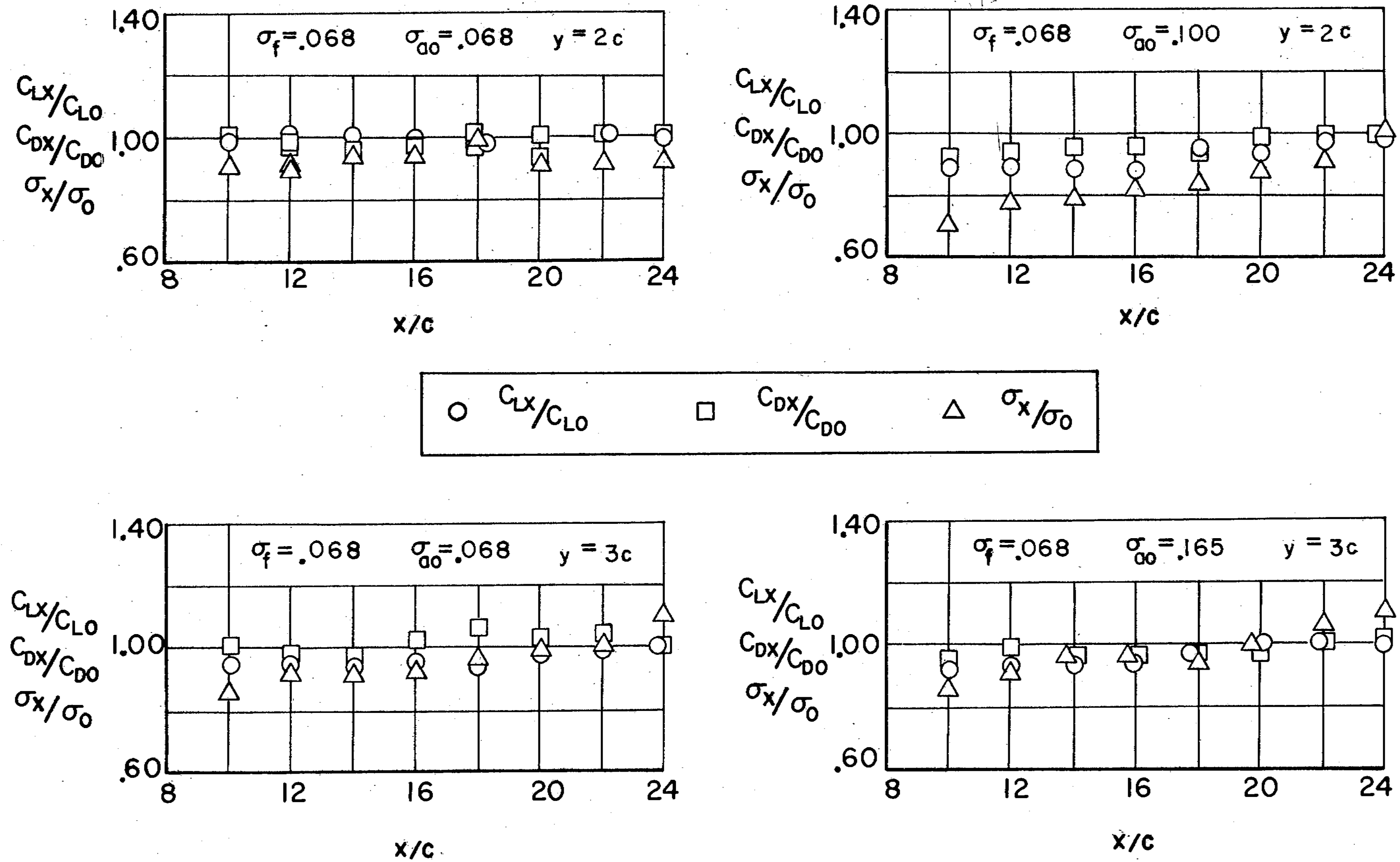

Fig. 15 - Interference Effects for Split Forward Foil System, Forced-Ventilated Foils, α = 14°, f = 1c, V = 14 fps, AR = 2

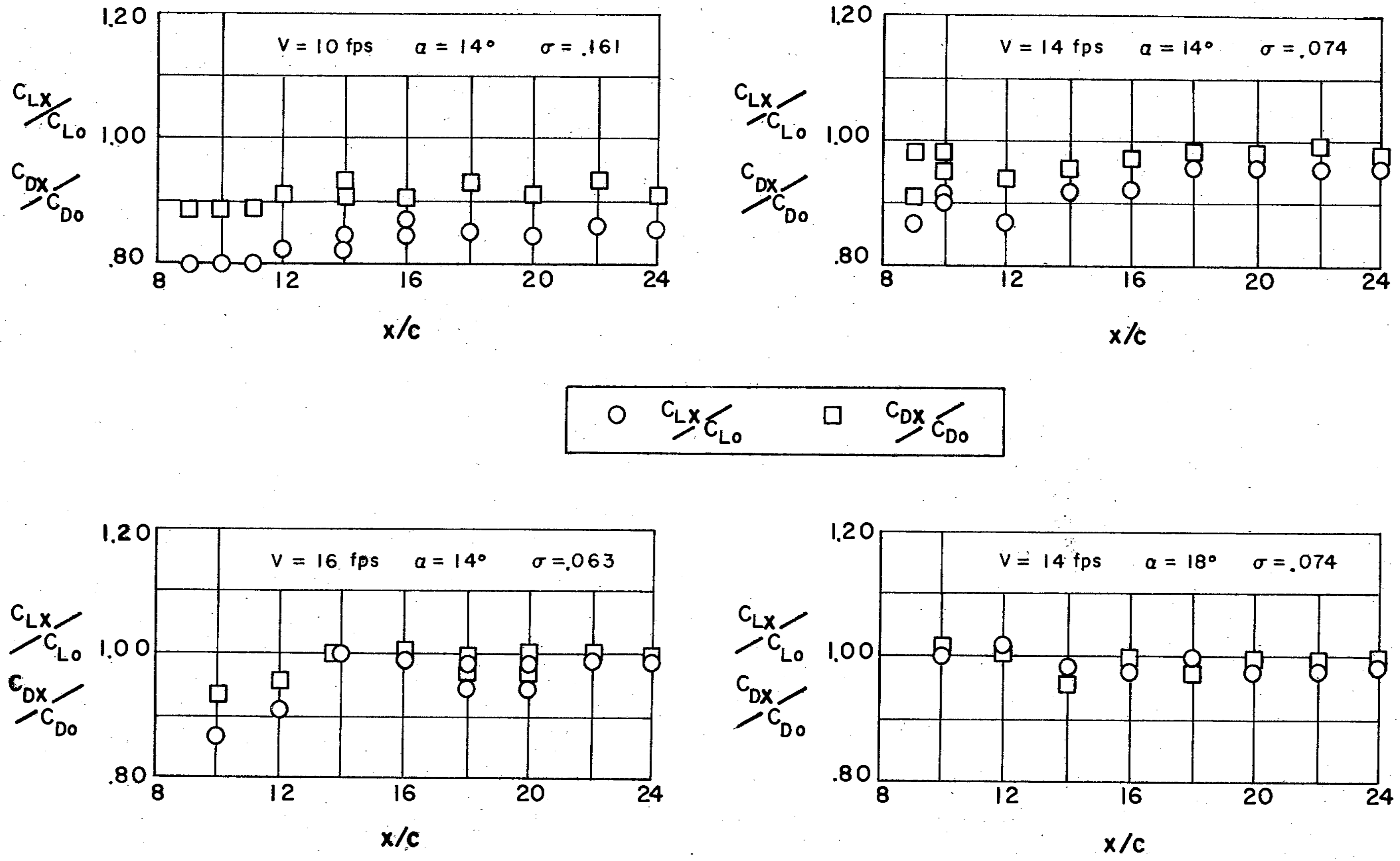

Fig. 16 - Interference Effects for Split Forward Foil System, Naturally Ventilated Foils, AR = 2, y = 0

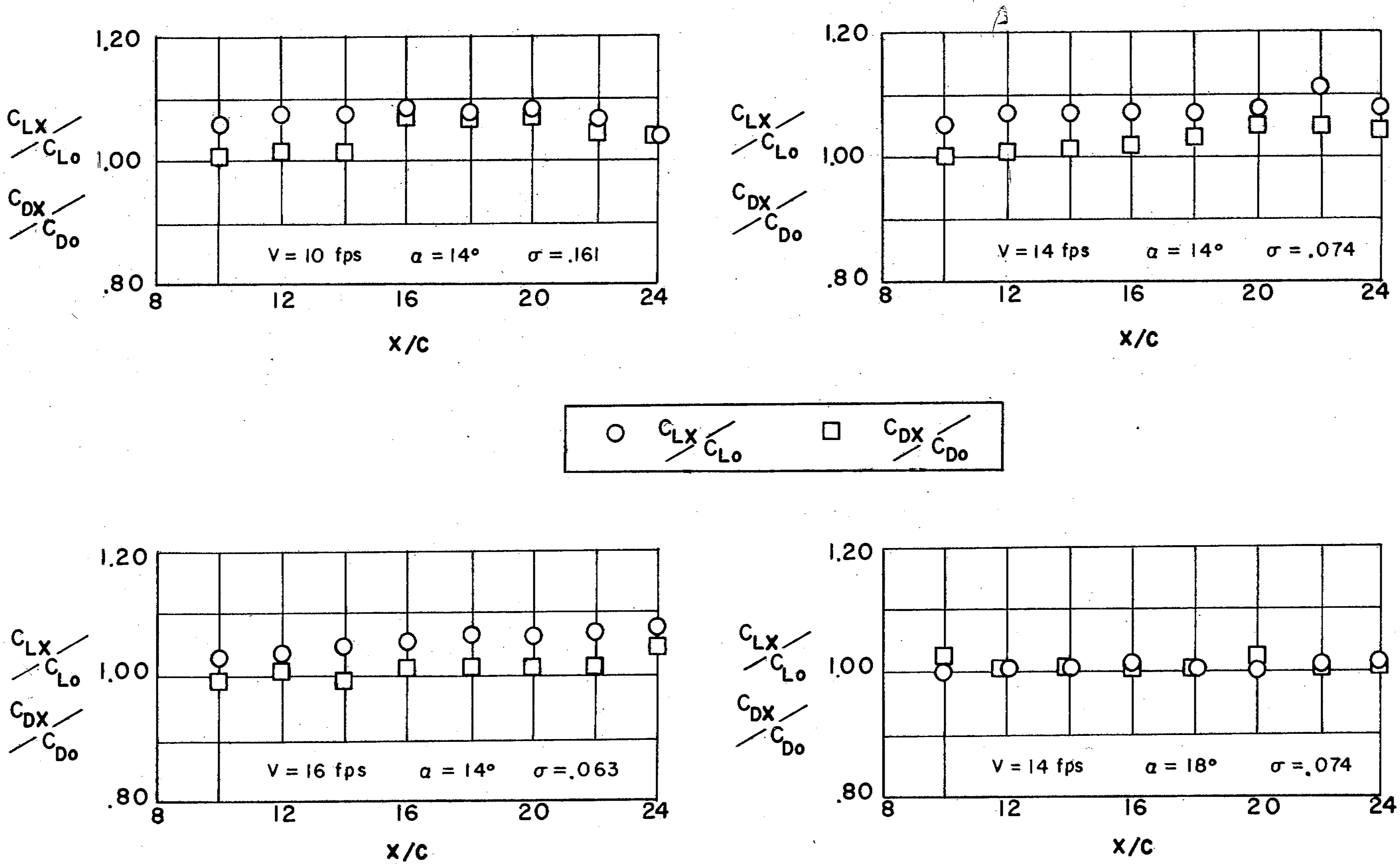

Fig. 17 - Interference Effects for Split Forward Foil System, Naturally Ventilated Foils, AR = 2, y = 2c

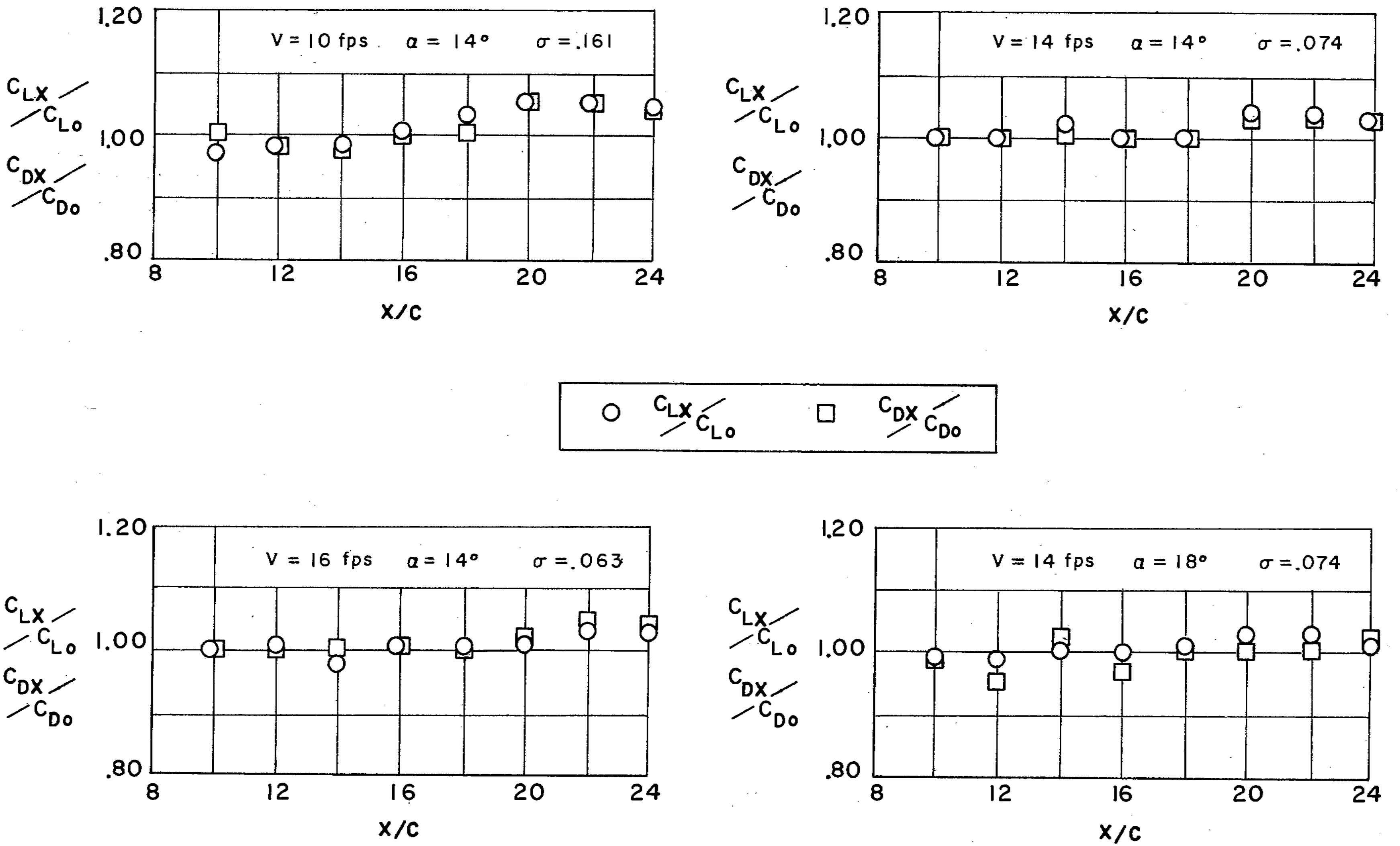

Fig. 18 - Interference Effects for Split Forward Foil System, Naturally Ventilated Foils, AR = 2, y = 4c

SPONSOR'S DISTRIBUTION LIST FOR TECHNICAL PAPER 50-B

of the St. Anthony Falls Hydraulic Laboratory

Copies	Organization
6	Chief of Naval Research, Department of the Navy, Washington, D. C. 20360, Attn: 3 - Code 438 1 - Code 461 1 - Code 463 1 - Code 466
1	Commanding Officer, Office of Naval Research, Branch Office, 495 Summer Street, Boston 10, Massachusetts.
1	Commanding Officer, Office of Naval Research, Branch Office, 219 S. Dearborn St., Chicago, Illinois 60604.
1	Commanding Officer, Office of Naval Research, Branch Office, 207 W. 24th Street, New York 11, New York.
25	Commanding Officer, Office of Naval Research, Branch Office, Navy No. 100, Box 39, Fleet Post Office, New York, New York.
1	Commanding Officer, Office of Naval Research, Branch Office, 1030 East Green Street, Pasadena 1, California.
1	Commanding Officer, Office of Naval Research, Branch Office, 1000 Geary Street, San Francisco 9, California.
6	Director, Naval Research Laboratory, Washington 25, D. C., Attn: Code 2027.
3	Chief, Bureau of Naval Weapons, Department of the Navy, Washington 25, D. C., Attn: 1 - Code RRRE 1 - Code RAAD 1 - Code RAAD-222
7	Chief, Bureau of Ships, Department of the Navy, Washington 25, D. C., Attn: 1 - Code 312 1 - Code 335 1 - Code 420 1 - Code 421 1 - Code 440 1 - Code 442 1 - Code 449
1	Chief, Bureau of Yards and Docks, Department of the Navy, Washington 25, D. C., Attn: Code D-400.
12	Commanding Officer and Director, David Taylor Model Basin, Washington 7, D. C., Attn: 1 - Code 500 1 - Code 513 1 - Code 520 1 - Code 525 1 - Code 526 1 - Code 526A

Copies	Organization
	1 - Code 530
	1 - Code 533
	1 - Code 580
	1 - Code 585
	1 - Code 589
	1 - Code 700
1	Commander, Naval Ordnance Test Station, China Lake, California, Attn: Code 753.
1	Commander, Naval Ordnance Test Station, Pasadena Annex, 3202 E. Foothill Boulevard, Pasadena 8, California, Attn: Code P508.
1	Commander, Portsmouth Naval Shipyard, Portsmouth, New Hampshire, Attn: Planning Department.
1	Commander, Boston Naval Shipyard, Boston, Massachusetts, Attn: Planning Department.
1	Commander, Pearl Harbor Naval Shipyard, Navy No. 128, Fleet Post Office, San Francisco, California, Attn: Planning Department.
1	Commander, San Francisco Naval Shipyard, San Francisco, California, Attn: Planning Department.
1	Commander, Mare Island Naval Shipyard, Vallejo, California, Attn: Planning Department.
1	Commander, New York Naval Shipyard, Brooklyn 1, New York, Attn: Planning Department.
1	Commander, Puget Sound Naval Shipyard, Bremerton, Washington, Attn: Planning Department.
1	Commander, Philadelphia Naval Shipyard, Philadelphia, Pennsylvania, Attn: Planning Department.
1	Commander, Norfolk Naval Shipyard, Portsmouth, Virginia, Attn: Planning Department.
1	Commander, Charleston Naval Shipyard, Charleston, South Carolina, Attn: Planning Department.
1	Commander, Long Beach Naval Shipyard, Long Beach 2, California, Attn: Planning Department.
1	Commander, U.S. Naval Weapons Laboratory, Dahlgren, Virginia, Attn: Planning Department.
1	Commander, U.S. Naval Ordnance Laboratory, White Oak, Maryland.
1	Commander, U.S. Naval Weapons Laboratory, Dahlgren, Virginia, Attn: Computation and Exterior Ballistics Laboratory (Dr. A. V. Hershey).
1	Superintendent, U.S. Naval Academy, Annapolis, Maryland, Attn: Library.
1	Superintendent, U.S. Naval Postgraduate School, Monterey, California.
1	Commandant, U.S. Coast Guard, 1300 E Street, N.W., Washington, D. C.
1	Secretary, Ship Structure Committee, U.S. Coast Guard Headquarters, 1300 E Street, N.W., Washington, D. C.

Copies	Organization
1	Commander, Military Sea Transportation Service, Department of the Navy, Washington 25, D. C.
1	Division of Ship Design, Maritime Administration, 441 G Street, N. W., Washington 25, D. C.
1	Superintendent, U.S. Merchant Marine Academy, Kings Point, Long Island, New York, Attn: Captain L. S. McCready.
1	Commanding Officer and Director, U.S. Navy Mine Defense Laboratory, Panama City, Florida.
1	Commanding Officer, NROTC and Naval Administrative Unit, Massachusetts Institute of Technology, Cambridge 39, Massachusetts.
1	Commander, Hdqs. U.S. Army Transportation Research and Development Command, Transportation Corps, Fort Eustis, Virginia, Attn: Marine Transportation Division.
1	Air Force Office of Scientific Research, Mechanics Division, Washington 25, D. C.
1	Commander, Wright Air Development Division, Aircraft Laboratory, Wright-Patterson Air Force Base, Ohio, Attn: Mr. W. Mykytow, Dynamics Branch.
1	Director of Research, Code RR, National Aeronautics and Space Administration, 600 Independence Avenue, S.W., Washington, D. C. 20546.
1	Director, Langley Research Center, Langley Station, Hampton, Virginia, Attn: Mr. I. E. Garrick.
1	Director, Langley Research Center, Langley Station, Hampton, Virginia, Attn: Mr. D. J. Marten.
1	Director, Engineering Science Division, National Science Foundation, Washington, D. C.
1	Director, National Bureau of Standards, Washington 25, D. C., Attn: Mr. J. M. Franklin.
1	Dr. G. B. Schubauer, Fluid Mechanics Section, National Bureau of Standards, Washington 25, D. C.
20	Defense Documentation Center, Cameron Station, Alexandria, Virginia.
1	Office of Technical Services, Department of Commerce, Washington 25, D. C.
1	Mr. Alfonso Alcadan L., Director, Laboratorio Nacional de Hydraulica, Antiguo Camino A Ancon, Casilla Postal 682, Lima, Peru.
1	Mr. T. A. Duncan, Lycoming Division, AVCO Corporation, 1701 K Street, N.W., Apartment 904, Washington, D. C.
1	Baker Manufacturing Company, Evansville, Wisconsin.
1	Professor S. Siestrunck, Bureau D'Analyse et de Recherche Appliquees, 47, Avenue Victor Cresson, Issy-les-Moulineaux, Seine, France.
1	Professor A. Acosta, California Institute of Technology, Pasadena 4, California.
1	Professor M. Plesset, California Institute of Technology, Pasadena 4, California.

Copies	Organization
1	Professor T. Y. Wu, California Institute of Technology, Pasadena 4, California.
1	Professor A. Powell, University of California, Los Angeles, California.
1	Dr. Maurice L. Albertson, Professor of Civil Engineering, Colorado State University, Fort Collins, Colorado 80521.
1	Professor J. E. Cermak, Colorado State University, Department of Civil Engineering, Fort Collins, Colorado.
1	Dr. Blaine R. Parkin, General Dynamics - Convair, P. O. Box 1950, San Diego 12, California.
1	Robert H. Oversmith, Chief of ASW/Marine Sciences, Mail Zone 6-107, General Dynamics - Convair, San Diego, California 92112.
1	Dr. Irving C. Statler, Head, Applied Mechanics Department, Cornell Aeronautical Laboratory, Inc., P. O. Box 235, Buffalo, New York 14221.
1	Mr. Richard P. White, Jr., Cornell Aeronautical Laboratory, 4455 Genessee Street, Buffalo, New York.
1	Professor W. R. Sears, Graduate School of Aeronautical Engineering, Cornell University, Ithaca, New York.
1	Mr. George H. Pederson, Curtiss-Wright Corporation, Wright Aeronautical Division, Wood-Ridge, New Jersey, Location CC-1 Engrg. Mezz.
1	Mr. G. Tedrew, Food Machinery Corporation, P. O. Box 367, San Jose, California.
1	General Applied Science Laboratory, Merrick and Stewart Avenues, Westbury, Long Island, New York, Attn: Dr. Frank Lane.
1	Mr. R. McCandliss, Electric Boat Division, General Dynamics Corporation, Groton, Connecticut.
1	Dr. A. S. Iberall, President, General Technical Services, Inc., 2640 Whiton Road, Cleveland 18, Ohio.
1	Gibbs and Cox, Inc., 21 West Street, New York, New York 10006.
1	Mr. Eugene F. Baird, Chief of Dynamic Analysis, Grumman Aircraft Engineering Corporation, Bethpage, Long Island, New York.
1	Mr. Robert E. Bower, Chief, Advanced Development, Grumman Aircraft Engineering Corporation, Bethpage, Long Island, New York.
1	Mr. William P. Carl, Grumman Aircraft Engineering Corporation, Bethpage, Long Island, New York.
1	Grumman Aircraft Engineering Corporation, Research Department, Plant 25, Bethpage, Long Island, New York 11714, Attn: Mr. Kenneth Keen.
1	Dr. O. Grim, Hamburgische Schiffbau-Versuchsanstalt, Bramfelder Strasse 164, Hamburg 33, Germany.
1	Dr. H. W. Lerbs, Hamburgische Schiffbau-Versuchsanstalt, Bramfelder Strasse 164, Hamburg 33, Germany.

Copies	Organization
1	Dr. H. Schwanecke, Hamburgische Schiffbau-Versuchsanstalt, Bramfelder Strasse 164, Hamburg 33, Germany.
1	Professor G. P. Weinblum, Director, Institute for Schiffbau, University of Hamburg, Berliner Tow 21, Hamburg, Germany.
1	Professor G. F. Carrier, Harvard University, Cambridge 38, Massachusetts.
1	Dr. S. F. Hoerner, 148 Busteed Drive, Midland Park, New Jersey.
1	Mr. P. Eisenberg, President, Hydronautics, Incorporated, Pindell School Road, Howard County, Laurel, Maryland.
1	Professor Carl Prohaska, Hydro-og Aerodynamisk Laboratorium, Lyngby, Denmark.
1	Professor L. Landweber, Iowa Institute of Hydraulic Research, State University of Iowa, Iowa City, Iowa.
1	Professor H. Rouse, Iowa Institute of Hydraulic Research, State University of Iowa, Iowa City, Iowa.
1	Professor S. Corrsin, Department of Mechanics, The Johns Hopkins University, Baltimore 18, Maryland.
2	Professor O. M. Phillips, Division of Mechanical Engineering, Institute for Cooperative Research, The Johns Hopkins University, Baltimore, Maryland.
1	Mr. Bill East, Lockheed Aircraft Corporation, California Division, Hydrodynamics Research, Burbank, California.
1	Mr. R. W. Kermeen, Lockheed Missiles and Space Company, Department 81-73/Bldg 538, P. O. Box 504, Sunnyvale, California.
1	Department of Naval Architecture and Marine Engineering, Room 5-228, Massachusetts Institute of Technology, 77 Massachusetts Avenue, Cambridge, Massachusetts 02139.
1	Professor M. A. Abkowitz, Massachusetts Institute of Technology, Cambridge 39, Massachusetts.
1	Professor H. Ashley, Massachusetts Institute of Technology, Cambridge 39, Massachusetts.
1	Professor A. T. Ippen, Massachusetts Institute of Technology, Cambridge 39, Massachusetts.
1	Professor M. Landahl, Massachusetts Institute of Technology, Cambridge 39, Massachusetts.
1	Dr. H. Reichardt, Director, Max-Planck Institut fur Stromungsforschung, Bottingerstrasse 6-8, Gottingen, Germany.
1	Professor R. B. Couch, University of Michigan, Ann Arbor, Michigan.
1	Professor W. W. Willmarth, University of Michigan, Ann Arbor, Michigan.
1	Midwest Research Institute, 425 Volker Boulevard, Kansas City, Missouri, Attn: Library.

Copies	Organization
1	Director, St. Anthony Falls Hydraulic Laboratory, University of Minnesota, Minneapolis 14, Minnesota.
1	Dr. C. S. Song, St. Anthony Falls Hydraulic Laboratory, University of Minnesota, Minneapolis 14, Minnesota.
1	Mr. J. M. Wetzel, St. Anthony Falls Hydraulic Laboratory, University of Minnesota, Minneapolis 14, Minnesota.
1	Head, Aerodynamics Division, National Physical Laboratory, Teddington, Middlesex, England.
1	Mr. A. Silverleaf, National Physical Laboratory, Teddington, Middlesex, England.
1	The Aeronautical Library, National Research Council, Montreal Road, Ottawa 2, Canada.
1	Dr. J. B. Van Manen, Netherlands Ship Model Basin, Wageningen, The Netherlands.
1	Professor John J. Foody, Chairman, Engineering Department, State University of New York, Maritime College, Bronx, New York 10465.
1	Professor J. Keller, Institute of Mathematical Sciences, New York University, 25 Waverly Place, New York 3, New York.
1	Professor J. J. Stoker, Institute of Mathematical Sciences, New York University, 25 Waverly Place, New York 3, New York.
1	Dr. T. R. Goodman, Oceanics, Incorporated, Technical Industrial Park, Plainview, Long Island, New York.
1	Professor J. William Holl, Department of Aeronautical Engineering, The Pennsylvania State University, Ordnance Research Laboratory, P. O. Box 30, University Park, Pennsylvania.
1	Dr. M. Sevik, Ordnance Research Laboratory, Pennsylvania State University, University Park, Pennsylvania.
1	Dr. George F. Wislicenus, Garfield Thomas Water Tunnel, Ordnance Research Laboratory, The Pennsylvania State University, P. O. Box 30, University Park, Pennsylvania 16801.
1	Professor E. J. Brunelle, Princeton University, Princeton, New Jersey.
1	Mr. David Wellinger, Hydrofoil Projects, Radio Corporation of America, Burlington, Massachusetts.
1	The RAND Corporation, 1700 Main Street, Santa Monica, California 90406, Attn: Library.
1	Professor R. C. DiPrima, Department of Mathematics, Rensselaer Polytechnic Institute, Troy, New York.
1	Mr. L. M. White, U.S. Rubber Company, Research and Development Department, Wayne, New Jersey.
1	Professor J. K. Lunde, Skipsmodelltanken, Trondheim, Norway.
1	Editor, Applied Mechanics Review, Southwest Research Institute, 8500 Culebra Road, San Antonio 6, Texas.

Copies	Organization
1	Dr. H. N. Abramson, Southwest Research Institute, 8500 Culebra Road, San Antonio 6, Texas.
1	Mr. G. Ransleben, Southwest Research Institute, 8500 Culebra Road, San Antonio 6, Texas.
1	Professor E. Y. Hsu, Stanford University, Stanford, California.
1	Dr. Byrne Perry, Department of Civil Engineering, Stanford University, Stanford, California 94305.
1	Dr. J. P. Breslin, Stevens Institute of Technology, Davidson Laboratory, Hoboken, New Jersey.
1	Mr. D. Savitsky, Stevens Institute of Technology, Davidson Laboratory, Hoboken, New Jersey.
1	Mr. S. Tsakonas, Stevens Institute of Technology, Davidson Laboratory, Hoboken, New Jersey.
1	Dr. Jack Kotik, Technical Research Group, Inc., Route 110, Melville, New York.
1	Dr. R. Timman, Department of Applied Mathematics, Technological University, Julianalaan 132, Delft, Holland.
1	Transportation Technical Research Institute, No. 1057-1 Chome, Mejiro-machi, Toshima-ku, Tokyo-to, Japan.
1	Dr. Grosse, Versuchsanstalt fur Wasserbau und Schiffbau, Schleuseninsel im Tiergarten, Berlin, Germany.
1	Dr. S. Schuster, Director, Versuchsanstalt fur Wasserbau und Schiffbau, Schleuseninsel im Tiergarten, Berlin, Germany.
1	Technical Library, Webb Institute of Naval Architecture, Glen Cove, Long Island, New York.
1	Professor E. V. Lewis, Webb Institute of Naval Architecture, Glen Cove, Long Island, New York.
1	Mr. C. Wigley, Flat 103, 6-9 Charterhouse Square, London E. C. 1, England.
1	Coordinator of Research, Maritime Administration, 441 G Street, N. W., Washington 25, D. C.

Unclassified
Security Classification

DOCUMENT CONTROL DATA - R&D

(Security classification of title, body of abstract and indexing annotation must be entered when the overall report is classified)

1. ORIGINATING ACTIVITY *(Corporate author)* St. Anthony Falls Hydraulic Laboratory, University of Minnesota	2a. REPORT SECURITY CLASSIFICATION Unclassified 2b. GROUP

3. REPORT TITLE

TANDEM INTERFERENCE EFFECTS FOR NONCAVITATING AND SUPERCAVITATING HYDROFOILS

4. DESCRIPTIVE NOTES *(Type of report and inclusive dates)*

Final report on this aspect of research

5. AUTHOR(S) *(Last name, first name, initial)*

Wetzel, Joseph M.

6. REPORT DATE	7a. TOTAL NO. OF PAGES	7b. NO. OF REFS
January 1965	55	5

8a. CONTRACT OR GRANT NO. Nonr 710(24) b. PROJECT NO. NR 062-052 c. d.	9a. ORIGINATOR'S REPORT NUMBER(S) Technical Paper No. 50-B 9b. OTHER REPORT NO(S) *(Any other numbers that may be assigned this report)*

10. AVAILABILITY/LIMITATION NOTICES

Qualified requestors may obtain copies of this report from DDC.

11. SUPPLEMENTARY NOTES	12. SPONSORING MILITARY ACTIVITY
	Office of Naval Research

13. ABSTRACT

Experimental data previously obtained at the St. Anthony Falls Hydraulic Laboratory relative to the tandem interference effects for noncavitating hydrofoils of finite span are compared with theory, and good agreement is shown to exist. The experimental studies were extended to include fully submerged, ventilated foils of finite span. Both forced and naturally ventilated foils were employed in various configurations. The surface waves generated by a forced-ventilated foil and the total interference effect of the forward foil or foils on the force and cavity characteristics of the aft foil were of particular interest.

14. KEY WORDS	LINK A		LINK B		LINK C	
	ROLE	WT	ROLE	WT	ROLE	WT
Hydrofoils						
Tandem Interference						
Noncavitating						
Supercavitating						
Free Surface Effects						
Finite Span						

INSTRUCTIONS

1. ORIGINATING ACTIVITY: Enter the name and address of the contractor, subcontractor, grantee, Department of Defense activity or other organization *(corporate author)* issuing the report.

2*a*. REPORT SECURITY CLASSIFICATION: Enter the overall security classification of the report. Indicate whether "Restricted Data" is included. Marking is to be in accordance with appropriate security regulations.

2*b*. GROUP: Automatic downgrading is specified in DoD Directive 5200.10 and Armed Forces Industrial Manual. Enter the group number. Also, when applicable, show that optional markings have been used for Group 3 and Group 4 as authorized.

3. REPORT TITLE: Enter the complete report title in all capital letters. Titles in all cases should be unclassified. If a meaningful title cannot be selected without classification, show title classification in all capitals in parenthesis immediately following the title.

4. DESCRIPTIVE NOTES: If appropriate, enter the type of report, e.g., interim, progress, summary, annual, or final. Give the inclusive dates when a specific reporting period is covered.

5. AUTHOR(S): Enter the name(s) of author(s) as shown on or in the report. Enter last name, first name, middle initial. If military, show rank and branch of service. The name of the principal author is an absolute minimum requirement.

6. REPORT DATE: Enter the date of the report as day, month, year; or month, year. If more than one date appears on the report, use date of publication.

7*a*. TOTAL NUMBER OF PAGES: The total page count should follow normal pagination procedures, i.e., enter the number of pages containing information.

7*b*. NUMBER OF REFERENCES: Enter the total number of references cited in the report.

8*a*. CONTRACT OR GRANT NUMBER: If appropriate, enter the applicable number of the contract or grant under which the report was written.

8*b*, 8*c*, & 8*d*. PROJECT NUMBER: Enter the appropriate military department identification, such as project number, subproject number, system numbers, task number, etc.

9*a*. ORIGINATOR'S REPORT NUMBER(S): Enter the official report number by which the document will be identified and controlled by the originating activity. This number must be unique to this report.

9*b*. OTHER REPORT NUMBER(S): If the report has been assigned any other report numbers *(either by the originator or by the sponsor)*, also enter this number(s).

10. AVAILABILITY/LIMITATION NOTICES: Enter any limitations on further dissemination of the report, other than those imposed by security classification, using standard statements such as:

(1) "Qualified requesters may obtain copies of this report from DDC."

(2) "Foreign announcement and dissemination of this report by DDC is not authorized."

(3) "U. S. Government agencies may obtain copies of this report directly from DDC. Other qualified DDC users shall request through
________________."

(4) "U. S. military agencies may obtain copies of this report directly from DDC. Other qualified users shall request through
________________."

(5) "All distribution of this report is controlled. Qualified DDC users shall request through
________________."

If the report has been furnished to the Office of Technical Services, Department of Commerce, for sale to the public, indicate this fact and enter the price, if known.

11. SUPPLEMENTARY NOTES: Use for additional explanatory notes.

12. SPONSORING MILITARY ACTIVITY: Enter the name of the departmental project office or laboratory sponsoring *(paying for)* the research and development. Include address.

13. ABSTRACT: Enter an abstract giving a brief and factual summary of the document indicative of the report, even though it may also appear elsewhere in the body of the technical report. If additional space is required, a continuation sheet shall be attached.

It is highly desirable that the abstract of classified reports be unclassified. Each paragraph of the abstract shall end with an indication of the military security classification of the information in the paragraph, represented as *(TS)*, *(S)*, *(C)*, or *(U)*.

There is no limitation on the length of the abstract. However, the suggested length is from 150 to 225 words.

14. KEY WORDS: Key words are technically meaningful terms or short phrases that characterize a report and may be used as index entries for cataloging the report. Key words must be selected so that no security classification is required. Identifiers, such as equipment model designation, trade name, military project code name, geographic location, may be used as key words but will be followed by an indication of technical context. The assignment of links, roles, and weights is optional.

Technical Paper No. 50, Series B
St. Anthony Falls Hydraulic Laboratory

TANDEM INTERFERENCE EFFECTS FOR NONCAVITATING AND SUPERCAVITATING HYDROFOILS, by J. M. Wetzel. January 1965. 55 pages incl. 18 illus. Contract Nonr 710(24).

Experimental data previously obtained at the St. Anthony Falls Hydraulic Laboratory relative to the tandem interference effects for noncavitating hydrofoils of finite span are compared with theory, and good agreement is shown to exist. The experimental studies were extended to include fully submerged, ventilated foils of finite span. Both forced and naturally ventilated foils were employed in various configurations. The surface waves generated by a forced-ventilated foil and the total interference effect of the forward foil or foils on the force and cavity characteristics of the aft foil were of particular interest.

Available from St. Anthony Falls Hydraulic Laboratory, University of Minnesota, at $1.75 per copy.

1. Hydrofoils
2. Tandem Interference
3. Noncavitating
4. Supercavitating
5. Free Surface Effects
6. Finite Span

I. Title
II. Wetzel, J. M.
III. St. Anthony Falls Hydraulic Laboratory
IV. Contract No. 710(24)

Unclassified

Technical Paper No. 50, Series B
St. Anthony Falls Hydraulic Laboratory

TANDEM INTERFERENCE EFFECTS FOR NONCAVITATING AND SUPERCAVITATING HYDROFOILS, by J. M. Wetzel. January 1965. 55 pages incl. 18 illus. Contract Nonr 710(24).

Experimental data previously obtained at the St. Anthony Falls Hydraulic Laboratory relative to the tandem interference effects for noncavitating hydrofoils of finite span are compared with theory, and good agreement is shown to exist. The experimental studies were extended to include fully submerged, ventilated foils of finite span. Both forced and naturally ventilated foils were employed in various configurations. The surface waves generated by a forced-ventilated foil and the total interference effect of the forward foil or foils on the force and cavity characteristics of the aft foil were of particular interest.

Available from St. Anthony Falls Hydraulic Laboratory, University of Minnesota, at $1.75 per copy.

1. Hydrofoils
2. Tandem Interference
3. Noncavitating
4. Supercavitating
5. Free Surface Effects
6. Finite Span

I. Title
II. Wetzel, J. M.
III. St. Anthony Falls Hydraulic Laboratory
IV. Contract No. 710(24)

Unclassified

Technical Paper No. 50, Series B
St. Anthony Falls Hydraulic Laboratory

TANDEM INTERFERENCE EFFECTS FOR NONCAVITATING AND SUPERCAVITATING HYDROFOILS, by J. M. Wetzel. January 1965. 55 pages incl. 18 illus. Contract Nonr 710(24).

Experimental data previously obtained at the St. Anthony Falls Hydraulic Laboratory relative to the tandem interference effects for noncavitating hydrofoils of finite span are compared with theory, and good agreement is shown to exist. The experimental studies were extended to include fully submerged, ventilated foils of finite span. Both forced and naturally ventilated foils were employed in various configurations. The surface waves generated by a forced-ventilated foil and the total interference effect of the forward foil or foils on the force and cavity characteristics of the aft foil were of particular interest.

Available from St. Anthony Falls Hydraulic Laboratory, University of Minnesota, at $1.75 per copy.

1. Hydrofoils
2. Tandem Interference
3. Noncavitating
4. Supercavitating
5. Free Surface Effects
6. Finite Span

I. Title
II. Wetzel, J. M.
III. St. Anthony Falls Hydraulic Laboratory
IV. Contract No. 710(24)

Unclassified

Technical Paper No. 50, Series B
St. Anthony Falls Hydraulic Laboratory

TANDEM INTERFERENCE EFFECTS FOR NONCAVITATING AND SUPERCAVITATING HYDROFOILS, by J. M. Wetzel. January 1965. 55 pages incl. 18 illus. Contract Nonr 710(24).

Experimental data previously obtained at the St. Anthony Falls Hydraulic Laboratory relative to the tandem interference effects for noncavitating hydrofoils of finite span are compared with theory, and good agreement is shown to exist. The experimental studies were extended to include fully submerged, ventilated foils of finite span. Both forced and naturally ventilated foils were employed in various configurations. The surface waves generated by a forced-ventilated foil and the total interference effect of the forward foil or foils on the force and cavity characteristics of the aft foil were of particular interest.

Available from St. Anthony Falls Hydraulic Laboratory, University of Minnesota, at $1.75 per copy.

1. Hydrofoils
2. Tandem Interference
3. Noncavitating
4. Supercavitating
5. Free Surface Effects
6. Finite Span

I. Title
II. Wetzel, J. M.
III. St. Anthony Falls Hydraulic Laboratory
IV. Contract No. 710(24)

Unclassified

Technical Paper No. 50, Series B
St. Anthony Falls Hydraulic Laboratory

TANDEM INTERFERENCE EFFECTS FOR NONCAVITATING AND SUPERCAVITATING HYDROFOILS, by J. M. Wetzel. January 1965. 55 pages incl. 18 illus. Contract Nonr 710(24).

Experimental data previously obtained at the St. Anthony Falls Hydraulic Laboratory relative to the tandem interference effects for noncavitating hydrofoils of finite span are compared with theory, and good agreement is shown to exist. The experimental studies were extended to include fully submerged, ventilated foils of finite span. Both forced and naturally ventilated foils were employed in various configurations. The surface waves generated by a forced-ventilated foil and the total interference effect of the forward foil or foils on the force and cavity characteristics of the aft foil were of particular interest.

Available from St. Anthony Falls Hydraulic Laboratory, University of Minnesota, at $1.75 per copy.

1. Hydrofoils
2. Tandem Interference
3. Noncavitating
4. Supercavitating
5. Free Surface Effects
6. Finite Span

I. Title
II. Wetzel, J. M.
III. St. Anthony Falls Hydraulic Laboratory
IV. Contract No. 710(24)

Unclassified

Technical Paper No. 50, Series B
St. Anthony Falls Hydraulic Laboratory

TANDEM INTERFERENCE EFFECTS FOR NONCAVITATING AND SUPERCAVITATING HYDROFOILS, by J. M. Wetzel. January 1965. 55 pages incl. 18 illus. Contract Nonr 710(24).

Experimental data previously obtained at the St. Anthony Falls Hydraulic Laboratory relative to the tandem interference effects for noncavitating hydrofoils of finite span are compared with theory, and good agreement is shown to exist. The experimental studies were extended to include fully submerged, ventilated foils of finite span. Both forced and naturally ventilated foils were employed in various configurations. The surface waves generated by a forced-ventilated foil and the total interference effect of the forward foil or foils on the force and cavity characteristics of the aft foil were of particular interest.

Available from St. Anthony Falls Hydraulic Laboratory, University of Minnesota, at $1.75 per copy.

1. Hydrofoils
2. Tandem Interference
3. Noncavitating
4. Supercavitating
5. Free Surface Effects
6. Finite Span

I. Title
II. Wetzel, J. M.
III. St. Anthony Falls Hydraulic Laboratory
IV. Contract No. 710(24)

Unclassified

Technical Paper No. 50, Series B
St. Anthony Falls Hydraulic Laboratory

TANDEM INTERFERENCE EFFECTS FOR NONCAVITATING AND SUPERCAVITATING HYDROFOILS, by J. M. Wetzel. January 1965. 55 pages incl. 18 illus. Contract Nonr 710(24).

Experimental data previously obtained at the St. Anthony Falls Hydraulic Laboratory relative to the tandem interference effects for noncavitating hydrofoils of finite span are compared with theory, and good agreement is shown to exist. The experimental studies were extended to include fully submerged, ventilated foils of finite span. Both forced and naturally ventilated foils were employed in various configurations. The surface waves generated by a forced-ventilated foil and the total interference effect of the forward foil or foils on the force and cavity characteristics of the aft foil were of particular interest.

Available from St. Anthony Falls Hydraulic Laboratory, University of Minnesota, at $1.75 per copy.

1. Hydrofoils
2. Tandem Interference
3. Noncavitating
4. Supercavitating
5. Free Surface Effects
6. Finite Span

I. Title
II. Wetzel, J. M.
III. St. Anthony Falls Hydraulic Laboratory
IV. Contract No. 710(24)

Unclassified

Technical Paper No. 50, Series B
St. Anthony Falls Hydraulic Laboratory

TANDEM INTERFERENCE EFFECTS FOR NONCAVITATING AND SUPERCAVITATING HYDROFOILS, by J. M. Wetzel. January 1965. 55 pages incl. 18 illus. Contract Nonr 710(24).

Experimental data previously obtained at the St. Anthony Falls Hydraulic Laboratory relative to the tandem interference effects for noncavitating hydrofoils of finite span are compared with theory, and good agreement is shown to exist. The experimental studies were extended to include fully submerged, ventilated foils of finite span. Both forced and naturally ventilated foils were employed in various configurations. The surface waves generated by a forced-ventilated foil and the total interference effect of the forward foil or foils on the force and cavity characteristics of the aft foil were of particular interest.

Available from St. Anthony Falls Hydraulic Laboratory, University of Minnesota, at $1.75 per copy.

1. Hydrofoils
2. Tandem Interference
3. Noncavitating
4. Supercavitating
5. Free Surface Effects
6. Finite Span

I. Title
II. Wetzel, J. M.
III. St. Anthony Falls Hydraulic Laboratory
IV. Contract No. 710(24)

Unclassified

Technical Paper No. 50, Series B
St. Anthony Falls Hydraulic Laboratory

TANDEM INTERFERENCE EFFECTS FOR NONCAVITATING AND SUPERCAVITATING HYDROFOILS, by J. M. Wetzel. January 1965. 55 pages incl. 18 illus. Contract Nonr 710(24).

Experimental data previously obtained at the St. Anthony Falls Hydraulic Laboratory relative to the tandem interference effects for noncavitating hydrofoils of finite span are compared with theory, and good agreement is shown to exist. The experimental studies were extended to include fully submerged, ventilated foils of finite span. Both forced and naturally ventilated foils were employed in various configurations. The surface waves generated by a forced-ventilated foil and the total interference effect of the forward foil or foils on the force and cavity characteristics of the aft foil were of particular interest.

Available from St. Anthony Falls Hydraulic Laboratory, University of Minnesota, at $1.75 per copy.

1. Hydrofoils
2. Tandem Interference
3. Noncavitating
4. Supercavitating
5. Free Surface Effects
6. Finite Span

I. Title
II. Wetzel, J. M.
III. St. Anthony Falls Hydraulic Laboratory
IV. Contract No. 710(24)

Unclassified

Technical Paper No. 50, Series B
St. Anthony Falls Hydraulic Laboratory

TANDEM INTERFERENCE EFFECTS FOR NONCAVITATING AND SUPERCAVITATING HYDROFOILS, by J. M. Wetzel. January 1965. 55 pages incl. 18 illus. Contract Nonr 710(24).

Experimental data previously obtained at the St. Anthony Falls Hydraulic Laboratory relative to the tandem interference effects for noncavitating hydrofoils of finite span are compared with theory, and good agreement is shown to exist. The experimental studies were extended to include fully submerged, ventilated foils of finite span. Both forced and naturally ventilated foils were employed in various configurations. The surface waves generated by a forced-ventilated foil and the total interference effect of the forward foil or foils on the force and cavity characteristics of the aft foil were of particular interest.

Available from St. Anthony Falls Hydraulic Laboratory, University of Minnesota, at $1.75 per copy.

1. Hydrofoils
2. Tandem Interference
3. Noncavitating
4. Supercavitating
5. Free Surface Effects
6. Finite Span

I. Title
II. Wetzel, J. M.
III. St. Anthony Falls Hydraulic Laboratory
IV. Contract No. 710(24)

Unclassified

Technical Paper No. 50, Series B
St. Anthony Falls Hydraulic Laboratory

TANDEM INTERFERENCE EFFECTS FOR NONCAVITATING AND SUPERCAVITATING HYDROFOILS, by J. M. Wetzel. January 1965. 55 pages incl. 18 illus. Contract Nonr 710(24).

Experimental data previously obtained at the St. Anthony Falls Hydraulic Laboratory relative to the tandem interference effects for noncavitating hydrofoils of finite span are compared with theory, and good agreement is shown to exist. The experimental studies were extended to include fully submerged, ventilated foils of finite span. Both forced and naturally ventilated foils were employed in various configurations. The surface waves generated by a forced-ventilated foil and the total interference effect of the forward foil or foils on the force and cavity characteristics of the aft foil were of particular interest.

Available from St. Anthony Falls Hydraulic Laboratory, University of Minnesota, at $1.75 per copy.

1. Hydrofoils
2. Tandem Interference
3. Noncavitating
4. Supercavitating
5. Free Surface Effects
6. Finite Span

I. Title
II. Wetzel, J. M.
III. St. Anthony Falls Hydraulic Laboratory
IV. Contract No. 710(24)

Unclassified

Technical Paper No. 50, Series B
St. Anthony Falls Hydraulic Laboratory

TANDEM INTERFERENCE EFFECTS FOR NONCAVITATING AND SUPERCAVITATING HYDROFOILS, by J. M. Wetzel. January 1965. 55 pages incl. 18 illus. Contract Nonr 710(24).

Experimental data previously obtained at the St. Anthony Falls Hydraulic Laboratory relative to the tandem interference effects for noncavitating hydrofoils of finite span are compared with theory, and good agreement is shown to exist. The experimental studies were extended to include fully submerged, ventilated foils of finite span. Both forced and naturally ventilated foils were employed in various configurations. The surface waves generated by a forced-ventilated foil and the total interference effect of the forward foil or foils on the force and cavity characteristics of the aft foil were of particular interest.

Available from St. Anthony Falls Hydraulic Laboratory, University of Minnesota, at $1.75 per copy.

1. Hydrofoils
2. Tandem Interference
3. Noncavitating
4. Supercavitating
5. Free Surface Effects
6. Finite Span

I. Title
II. Wetzel, J. M.
III. St. Anthony Falls Hydraulic Laboratory
IV. Contract No. 710(24)

Unclassified